Hamaratoglu et al., 2006). The Hippo signaling cascade is a critical regulator of organ size in *Drosophila* as well as in mammals (Dong et al., 2007). In the conditional transgenic mouse model, the dysregulation of the pathway leads to tumorigenesis (Zhang et al., 2010). Considering Merlin and downstream components of the Hippo cascade, SAV1 (Salvador 1) and LATS2 (large tumor suppressor 2), 75% of MM cell lines had genetic inactivation of at least one of these three proteins (Murakami et al., 2011). Merlin inhibits the transcriptional coactivation activity of Yes-associated protein (YAP) by inducing phosphorylation and cytoplasmic retention of YAP (Yokoyama et al., 2008). YAP accumulation in the nucleus is also observed in MMs accompanied by mutation or deletion of *LATS2* (Murakami et al., 2011). YAP is a possible oncogene that associates with TEAD (TEA domain family member), a transcription factor, and exerts biological functions such as gene expression stimulation, cell growth, anchorage-independent cell growth, and epithelial-mesenchymal transition (Vassilev et al., 2001; Zhao et al., 2008, 2009).

TGF-β was originally identified as a protein that mediates the transformation of nonneoplastic rat kidney and murine AKR-2B fibroblasts (de Larco and Todaro, 1978; Moses et al., 1981; Anzano et al., 1983). TGF-β can induce extremely variable responses depending on the cell type, mainly through the Smad2/3-dependent pathway. For example, TGF-β induces growth arrest and apoptosis in epithelial cells; it can also activate fibroblasts. Subsequent studies further revealed that TGF-β acts as a tumor suppressor in premalignant cells as well as cells progressing through the early stages of carcinogenesis; furthermore, it exerts prooncogenic effects in metastatic tumors (Roberts and Wakefield, 2003; Massagué, 2008). TGF-β is a powerful cytokine produced by many different cell types, with effects on multiple cell types, and because of this complexity, signaling in each cell and context should be carefully studied.

Upon TGF-β stimulation, Smad2 and Smad3 form complexes with Smad4 and accumulate in the nucleus (Massagué et al., 2005). p300, a transcriptional co-activator, binds with Smad3 and Smad2 and enhances Smad-induced transactivation of target genes (Nishihara et al., 1998). Recruitment of p300 frequently plays a core role not only in enhancing transactivation but also in binding other proteins to stabilize protein complexes (Fujii et al., 2006).

Mesothelial cells were reported to demonstrate an increase in DNA synthesis after TGF-β stimulation (Gabrielson et al., 1988), and both normal human mesothelial cells and MM cell lines secrete TGF-β (Gerwin et al., 1987). Furthermore, a soluble TGF-β type II receptor inhibitor and a TGF-β type I receptor kinase inhibitor (SM16) were shown to inhibit the growth of murine MM tumors injected into the flanks of mice through the reactivation of antitumor immune responses (Suzuki et al., 2004, 2007).

Given the involvement of genetic inactivation of components of the Hippo pathway in 75% of mesotheliomas and previous evidence for a protumorigenic role for the TGF-β pathway, we examined the relationship between these two pathways to further understand the molecular mechanisms underlying mesothelioma genesis. Cross talk between the Hippo and TGF-β and BMP (bone morphogenetic protein) signaling pathways has been previously reported (Varelas et al., 2008, 2010; Alarcón et al., 2009). TAZ controls nucleocytoplasmic localization of Smad2/3–Smad4 complexes and regulates the nuclear accumulation of Smad complexes (Varelas et al., 2008). Furthermore, TAZ and YAP dictate the localization of active Smad complexes during mouse embryogenesis (Varelas et al., 2010). YAP is also known to strongly bind to Smad1 and support Smad1-dependent transcription and is required for BMP suppression of neural differentiation in mouse embryonic stem cells (Alarcón et al., 2009). However, whether the cross talk between Hippo and TGF-β signaling plays an important role in tumorigenesis has not been elucidated. We found that YAP and Smad3 interact at the transcription regulation level through participants of other related transcription cofactors, forming a complex in the *connective tissue growth factor* (*CTGF*) promoter region and thereby enhancing CTGF expression. This evidence shows that the cross talk between the Hippo and TGF-β pathway directly controls prooncogenic effects in malignancy. We further show that antagonism of the TGF-β pathway and CTGF expression can prolong the survival of mice with MM tumor xenografts, suggesting new approaches for the treatment of MM.

RESULTS

The TGF-β–Smad pathway is activated in clinical samples of human mesothelioma and regulates proliferation and extracellular matrix (ECM) production in MM cells in vitro

To assess the involvement of the TGF-β pathway in MM tumor growth, we performed immunohistochemical analysis in 24 tissue specimens obtained from patients to determine the p-Smad2 level and evaluate whether MM cells receive TGF-β signaling during their growth. In all 24 samples, which were subtyped into three major categories, epithelioid (12 patients), biphasic (3 patients), and sarcomatoid (7 patients), p-Smad2 staining was strongly observed in nuclei. This suggested that the constitutive activation of TGF-β is important for MM tumor development (Fig. 1 A and see Table 2). Histological subtype is a significant prognostic factor associated with longer survival because the median survival for patients with epithelioid tumors is 16.3 mo, which is longer than that for patients with biphasic tumors (9.5 mo) and sarcomatoid tumors (6.1 mo; Flores et al., 2007). Samples from all three subtypes exhibited the same level of p-Smad2 nuclear staining, indicating that the activation of the TGF-β pathway is maintained across different grades of malignancies, whereas normal pleural mesothelial cells did not exhibit significant p-Smad2 signals (Fig. 1 B, top, arrowheads). Interestingly, the nuclei of reactive pleural mesothelial cells, which were adjacent to the mesothelioma, having cuboidal appearance may be under serosal stimulation and were positively stained by p-Smad2, suggesting that the surrounding tissues were also affected by paracrine TGF-β signaling (Fig. 1 B, bottom).

TGF-β promotes proliferation and ECM production in normal and malignant mesothelial cells

To examine whether TGF-β signaling affects monolayer cell growth, we compared cell growth by counting cell number after exposing cells to a TGF-β type I receptor kinase inhibitor, SD-208. MeT-5A is a nonmalignant human pleural mesothelial cell line immortalized by SV40 early region DNA (Ke et al., 1989). Phosphorylation of Smad3 by TGF-β peaked around 1 h and gradually decreased later in the MeT-5A cells and MM cell lines (Fig. S1 A). The proliferation and the activation of MeT-5A cells and MM cell lines, as well as the Smad-dependent pathway induced by TGF-β in these cells were effectively suppressed by TGF-β type I receptor kinase inhibitor (Fig. 1 C and Fig. S1, B and C). To further assess

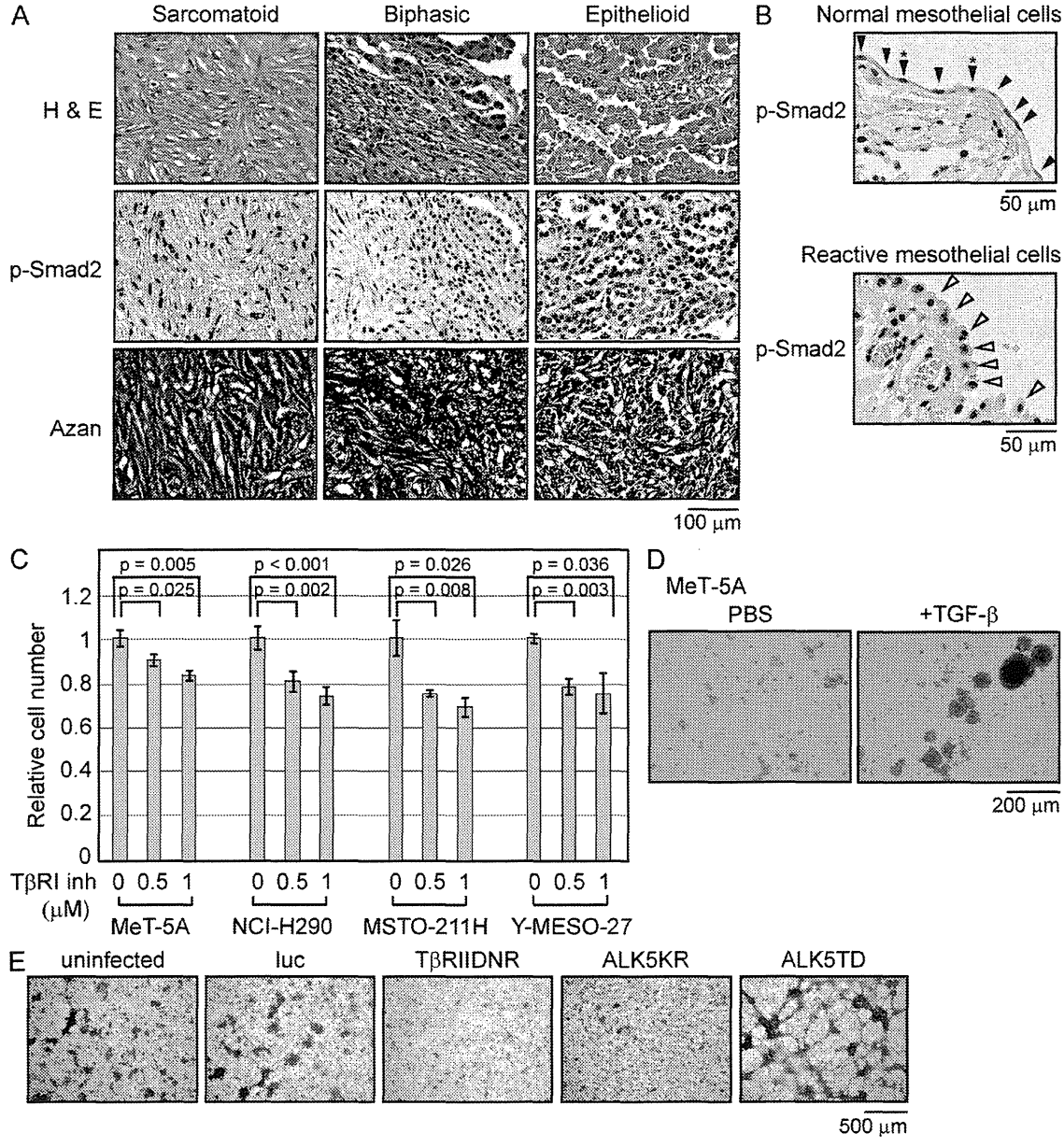

Figure 1. TGF-β signaling affects the growth of human MM cells. (A) Immunohistochemical staining for p-Smad2 of MM tissues derived from patients. Three representative sections, namely sarcomatoid, biphasic, and epithelioid subtype tumors, are shown. Azan staining was performed to visualize collagen fibers. H&E, hematoxylin and eosin. (B) Immunohistochemical staining for p-Smad2 in normal mesothelial cells (closed arrowheads) from normal lungs and reactivated normal mesothelial cells (open arrowheads) adjacent to MM tumors. Asterisks show cells with positive nuclear staining in normal mesothelial cells. (C) Cell numbers were counted 3 d after treatment with TGF-β type I receptor kinase inhibitor (SD-208). Results are expressed as mean ± SEM and are representative of three independent assays. (D) Soft agar colony formation assay was performed using MeT-5A cells treated with 4 ng/ml TGF-β for 7 d. The panel is representative of three independent assays. (E) NCI-H290 cells were infected with the indicated lentiviral expression vectors and stained with Giemsa after 14 d. HA-tagged luciferase (luc) was used as a control. The panel is representative of three independent assays. TβRIIDNR, dominant-negative form of the TGF-β type II receptor; ALK5KR, dominant-negative form of the TGF-β type I receptor; ALK5TD, constitutively activated TGF-β type I receptor.

Table 1. Common genes responsive to TGF-β in MeT-5A and Y-MESO-27 cells

Symbol	Description
MeT-5A and Y-MESO-27 common genes up (>1.5fold)	
CSF1R	colony-stimulating factor 1 receptor
SNAI1	snail homologue 1
*LOX**	lysyl oxidase
RASGRP1	RAS guanyl-releasing protein 1
*MMP2**	matrix metallopeptidase 2
*ITGA11**	integrin, alpha 11
SERPINE1	plasminogen activator inhibitor type 1
BMP6	bone morphogenetic protein 6
GDF6	growth differentiation factor 6
*COL1A1**	Prepro-alpha1(I) collagen
EDN1	endothelin 1
*COL1A2**	collagen, type I, alpha 2
MFAP4	microfibrillar-associated protein 4
SERPINE2	plasminogen activator inhibitor type 1, member 2
*COL20A1**	collagen, type XX, alpha 1
*COL5A1**	collagen, type V, alpha 1
*ITGB3**	integrin, beta 3
LTBP2	latent transforming growth factor beta binding protein 2
SMAD7	SMAD family member 7
*COL7A1**	collagen, type VII, alpha 1
SKIL	SKI-like oncogene
*COL4A1**	collagen, type IV, alpha 1
TGFB1	transforming growth factor, beta 1
*ITGAV**	integrin, alpha V (vitronectin receptor)
IGFBP3	insulin-like growth factor binding protein 3
*COL4A4**	collagen, type IV, alpha 4
CDH11	cadherin 11, type 2, OB-cadherin (osteoblast)
GADD45B	growth arrest and DNA-damage-inducible, beta
ADAM12	ADAM metallopeptidase domain 12
BMPR2	bone morphogenetic protein receptor, type II
*ITGA1**	integrin, alpha 1
*COL16A1**	collagen, type XVI, alpha 1
MDAC1	MDAC1
TGFB2	transforming growth factor, beta 2
EGR2	early growth response 2
*CTGF**	connective tissue growth factor
ID3	inhibitor of DNA binding 3
*FN1**	fibronectin
MeT-5A and Y-MESO-27 common genes down (<0.67-fold)	
IL6R	interleukin 6 receptor
VCAM1	vascular cell adhesion molecule 1
CASP1	caspase 1, apoptosis-related cysteine peptidase
IL12A	interleukin 12, alpha
IL1A	interleukin 1, alpha
IL7	interleukin 7
FAS	TNF receptor superfamily, member 6
*MMP26**	matrix metallopeptidase 26
FGF23	fibroblast growth factor 23
CAMK2A	calcium/calmodulin-dependent protein kinase II alpha
NEDD4L	neural precursor cell expressed, developmentally down regulated 4-like
*COL24A1**	collagen, type XXIV, alpha 1
TGFA	transforming growth factor, alpha
CAMK2D	calcium/calmodulin-dependent protein kinase II delta
TLR3	toll-like receptor 3
BCL2	B-cell CLL/lymphoma 2

MeT-5A and Y-MESO-27 cells were treated with TGF-β for 24 h. Total RNA was extracted and subjected to microarray analysis. The genes encoding ECM-related protein are indicated by an asterisk.

the biological activity of TGF-β in mesothelial cells, we performed an anchorage-independent cell proliferation assay with MeT-5A cells. After 7 d, colony formation was observed, showing the innate response of MeT-5A cells to TGF-β, which promotes colony formation similarly to that observed in fibroblasts (Fig. 1 D). Using a lentiviral vector system, we examined whether TGF-β signaling could modulate focus formation in NCI-H290 cells, an MM cell line (Fig. 1 E). Examination of the foci formed after 14 d showed a prominent decrease in the number of foci formed in cells expressing dominant-negative forms of the TGF-β type I and type II receptors. Conversely, cells with constitutive activation of the TGF-β type I receptor showed aggressive formation of foci, suggesting that TGF-β signaling affects the oncogenic property of mesothelioma cells.

To further investigate the molecular consequences of TGF-β pathway activation in mesothelioma cells, we performed cDNA microarray analysis to elucidate alterations in gene expression profiles after TGF-β treatment in MeT-5A and Y-MESO-27 cells (Table 1). Looking for overlap in the gene expression profiles, we found that 54 genes were regulated more than 1.5-fold by TGF-β in both cell types after 24 h of treatment. 42% of the commonly up-regulated genes (16/38) in TGF-β–treated MeT-5A cells and Y-MESO-27 cells were classified as ECM-related proteins. Changes in the expression profiles of representative genes (e.g., *MMP2*, *CTGF*, *COL1A1*, and *TGF-β*) were confirmed by real-time RT-PCR (Fig. S1, D and E).

YAP is critical for TGF-β induction of a small number of target genes

Genetic alteration of the tumor suppressor gene *NF2* and downstream components of the Hippo pathway, *SAV1* and *LATS2*, were observed in 75% of MM tumors (Murakami et al., 2011). This suggests that the disturbance of the Hippo pathway is strongly associated with the development of mesothelioma. Merlin, a protein encoded by *NF2*, *SAV1*, or *LATS*, negatively regulates YAP, whose oncogenic property has been recently reported (Wang et al., 2009). Dephosphorylated YAP translocates into the nucleus, where it binds to TEAD and activates the transcription of target genes. Merlin inhibits the

transcriptional coactivation activity of YAP by inducing phosphorylation and cytoplasmic retention of YAP (Yokoyama et al., 2008). Furthermore, genome-wide comprehensive genomic hybridization analysis of 22 MM specimens from patients showed that there is high copy amplification of 11q22 regions containing the *YAP* oncogene (Taniguchi et al., 2007). Thus, many genetic alterations in the Hippo pathway that have been seen in mesothelioma converge to increase YAP activity.

To analyze the possible alteration in TGF-β response in mesothelioma cells caused by defects in the Hippo pathway, we suppressed endogenous YAP expression using short hairpin RNA (shRNA) vectors in NCI-H290 cells, which have a genetic deletion of *NF2*. *YAP* messenger RNA (mRNA) expression was successfully down-regulated in shYAP-transfected cells without any alteration after treatment of TGF-β for either 2 or 24 h. *YAP* expression was not affected by TGF-β treatment in MM cells (Fig. 2 A). Because YAP is a known transcriptional modulator, we investigated the effect of *YAP* down-regulation on mRNA levels of genes regulated by TGF-β. Interestingly, genes regulated by TGF-β could be categorized into one of three groups. The expression of *fibronectin* and *COL1A1* did not immediately change; however, these genes were later activated by TGF-β, suggesting that they may be the target of a secondary response to TGF-β.

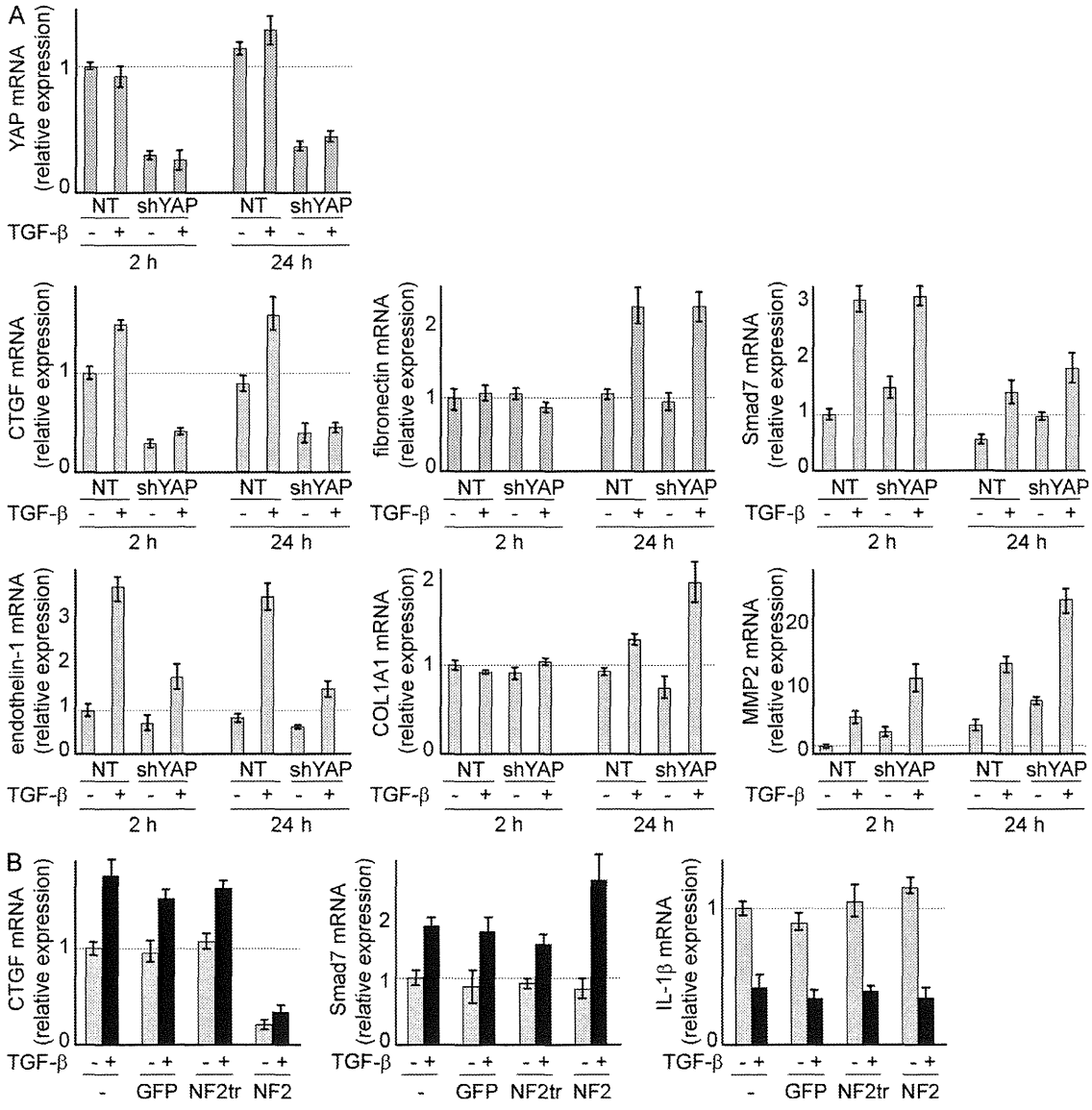

Figure 2. The CTGF expression level was modulated by the TGF-β and Hippo pathways in MM cells. (A) NCI-H290 cells, which show homologous deletion of *NF2* with concomitant YAP translocation to the nucleus, were transfected with plasmids containing shYAP. After 48 h of puromycin selection, TGF-β was added, followed by mRNA extraction after 2 and 24 h to perform real-time RT-PCR to evaluate gene expression. A plasmid with a nontarget sequence (NT) was used as the control. (B) Lentiviral vectors containing full-length and truncated NF2 that lack the ability to phosphorylate YAP on Ser 127 were used to infect NCI-H290 cells. Real-time RT-PCR was performed using mRNA extracted 2 h after TGF-β treatment. −, untreated or uninfected; NF2tr, truncated NF2. (A and B) Results are expressed as mean ± SEM and are representative of three independent assays.

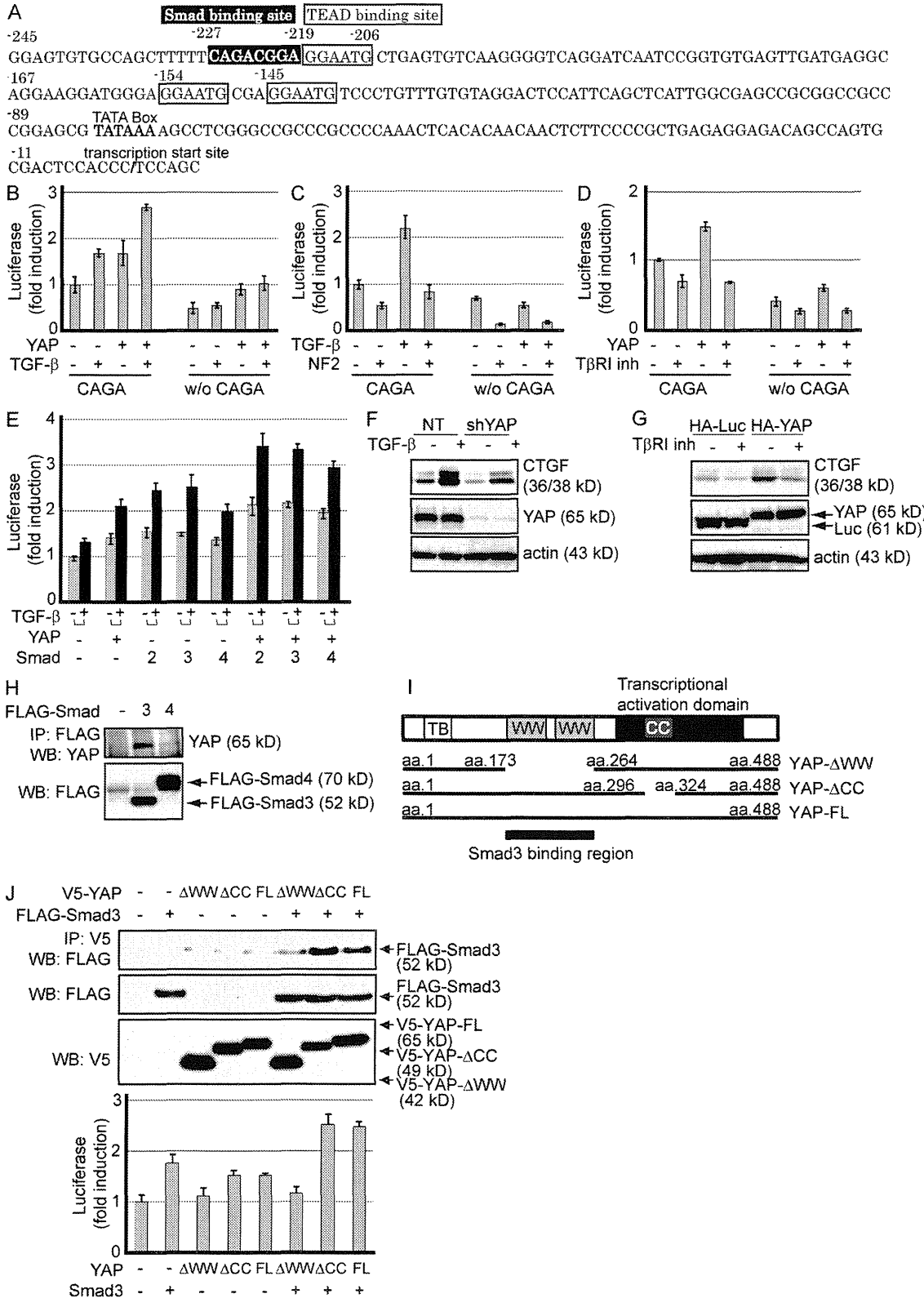

Figure 3. Smad3 interacts with YAP and enhances the transactivation activity of the *CTGF* promoter. (A) The human *CTGF* promoter region contains a Smad-binding site (−227 to −220) and a TEAD-binding site (−219 to −214) adjacent to each other. A luciferase reporter plasmid was linked to the *CTGF* promoter with (*CAGA*, −245 to 16) or without (w/o *CAGA*, −206 to 16) the Smad/TEAD-binding sites indicated. (B–D) NCI-H290 cells were transfected with *CTGF*-luciferase reporter plasmids with or without the Smad/TEAD-binding sites, together with the indicated plasmids. After 24 h, either the TGF-β or TβRI inhibitor was added to

Smad7 and *MMP2* were up-regulated by TGF-β within 2 h, but *YAP* depletion did not affect this activation. *CTGF* and *endothelin-1* were activated by TGF-β within 2 h, and this activation was suppressed by knockdown of endogenous *YAP*. Surprisingly, the number of functionally known genes identified by expression microarray, up-regulated in control versus TGF-β by >1.5-fold and also down-regulated in nontarget shRNA with TGF-β versus shYAP with TGF-β by <0.67-fold, was limited to these two genes in NCI-H290 cells (unpublished data). The aforementioned observations suggest that *YAP* does not influence the expression of all TGF-β target genes but does affect the transactivation of select genes. To confirm this result, NCI-H290 cells were infected with lentivirus vector carrying *GFP*, full-length *NF2*, or *NF2* with the truncated FERM (four-point-one/ezrin/radixin/moesin) domain. FERM truncation resulted in loss in the ability to phosphorylate YAP on Ser 127 (Yokoyama et al., 2008). Although neither *Smad7* up-regulation nor *IL-1β* down-regulation was affected, irrespective of TGF-β treatment, *CTGF* was greatly suppressed by *NF2* overexpression (Fig. 2 B).

YAP associates with Smad2/3 and synergistically enhances the transactivation of CTGF

TGF-β is known to positively regulate CTGF expression through Smad activation in NIH 3T3 fibroblasts (Holmes et al., 2001) and induces fibrosis in vivo. YAP binds to TEAD, and it is recruited to the putative TEAD-binding site that resides on the *CTGF* promoter (Zhao et al., 2008). We found that the *CTGF* promoter contains both a TEAD-binding site and a consensus Smad-binding site adjacent to each other (Fig. 3 A). Smad3 is a crucial mediator of TGF-β signaling, directly activating genes through Smad3/Smad4 DNA-binding motifs in mouse embryo fibroblasts (Yang et al., 2003; Roberts et al., 2006). To examine whether the TGF-β pathway and YAP may regulate the transcriptional activity of *CTGF*, we generated *CTGF* promoters containing or lacking this Smad/TEAD-binding site linked to luciferase. Treatment with TGF-β as well as overexpression of YAP enhanced the transcriptional activity of the *CTGF* promoter with the Smad-binding site in NCI-H290 cells. Deletion of the Smad/TEAD-binding site weakened basal promoter activities and responses to YAP (Fig. 3 B). The slight induction by TGF-β was possibly through TEAD-binding sites and might be the effects of the complex formation described in Fig. 4. Merlin, a protein encoded by *NF2*, suppresses TGF-β–induced activation, indicating the involvement of the Hippo signaling pathway in *CTGF* promoter activation by TGF-β (Fig. 3 C). On the contrary, TGF-β type I receptor kinase inhibitor blocked the transactivation by YAP (Fig. 3 D). Transfection of vectors carrying Smad2, Smad3, and Smad4 together with YAP enhanced the transcriptional activity of the *CTGF* promoter, which was further activated by TGF-β treatment (Fig. 3 E). The data suggest that Smad3 and YAP can synergize to up-regulate CTGF expression.

To confirm these results at the protein level, we overexpressed YAP in MM cells and investigated whether CTGF protein expression was modulated by the TGF-β pathway and YAP. Depletion of endogenous YAP suppressed CTGF protein expression in both cell lines, irrespective of TGF-β treatment (Fig. 3 F). Conversely, TGF-β type I receptor kinase inhibitor suppressed YAP-enhanced CTGF expression (Fig. 3 G). These results further support the possible involvement of two distinct pathways in CTGF regulation.

Functional and physical associations between Smads and WW domain–containing proteins such as TAZ and YAP have been demonstrated, and these associations were implicated in the transcription of multiple target genes (Varelas et al., 2008; Alarcón et al., 2009). We found that YAP binds to Smad3 but not to Smad4 (Fig. 3 H). To identify the requisite domain in the Smad3–YAP interaction, we used YAP deletion constructs, which lacked either WW or coiled-coil (CC) domains (Fig. 3 I). Smad3 could be coimmunoprecipitated with YAP-ΔCC, but a prominent decrease in binding was observed with YAP-ΔWW, suggesting that the WW domain is important for YAP binding to Smad3 (Fig. 3 J, top). In agreement with this result, although YAP-ΔCC could enhance the transcriptional activity of the *CTGF* promoter, YAP-ΔWW failed to augment this activity (Fig. 3 J, bottom). These data suggest the functional interaction through the YAP-WW domain with Smad3 in regulating CTGF expression.

YAP, Smad3, TEAD, and p300 comprise a common complex

Although the aforementioned results suggest physical binding and functional interactions between YAP and Smad3, the affinity of these proteins are not strong compared with the interaction of YAP with Smad1, as previously shown in HEK293T cells (Alarcón et al., 2009). To address this issue, we assessed the possible involvement of components in complex

the medium and incubated for an additional 24 h. Fold induction of transcriptional response relative to untreated cells is shown. Results are expressed as mean ± SEM and are representative of three independent assays. (E) Effects of TGF-β treatment on the activation of the *CTGF* promoter by YAP and Smads in NCI-H290 cells. Fold induction of transcriptional response relative to untreated cells is shown. Results are expressed as mean ± SEM and are representative of three independent assays. (F) Y-MESO-27 cells were lentivirally infected with either nontarget (NT) or YAP shRNA (shYAP) vector, followed by treatment with TGF-β type I receptor kinase inhibitor. Protein levels were determined by Western blotting. (G) Y-MESO-27 cells were lentivirally infected to express YAP protein and were treated with TGF-β. A lentivirus vector containing HA-luciferase was used as a control. Protein levels were determined by Western blotting. (H) HEK293 cells were transiently transfected with flag-tagged Smad vectors, and lysates were subjected to immunoprecipitation (IP), followed by Western blotting (WB) with anti-YAP antibody. Expression levels of exogenous Smads were confirmed in the bottom panel. (I) Schematic representation of the deletion constructs of YAP. CC, CC domains; FL, full length; TB, TEAD-binding domain; WW, WW domains. (J) HEK293 cells were transiently transfected with the indicated plasmids and subjected to immunoprecipitation. Western blotting was performed to confirm the expression level of YAP and Smad3 (top). NCI-H290 cells were transfected with the *CTGF*-luciferase reporter plasmid and combinations of Smad3 and YAP deletion constructs (bottom). Results are mean ± SEM and are representative of three independent assays.

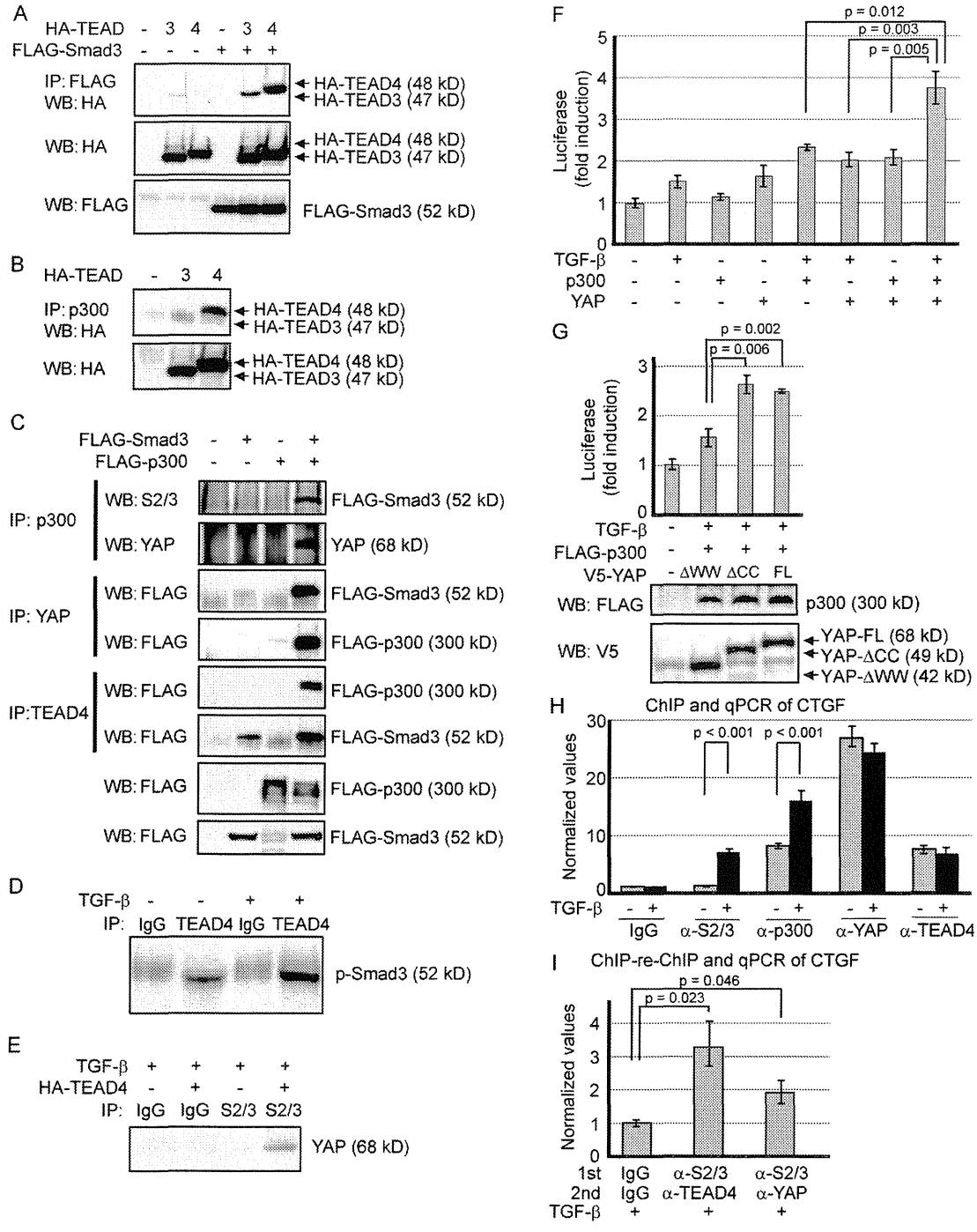

Figure 4. Smad3, YAP, TEAD, and p300 are components of a functional complex on the *CTGF* promoter. (A and B) HEK293 cells were transiently co-transfected with indicated plasmids, and lysates were subjected to immunoprecipitation (IP) followed by Western blotting (WB). (C) HEK293 cells were transfected with expression vectors as indicated. Cell lysates were divided and subjected to immunoprecipitation using p300, YAP, and TEAD4 antibodies. Samples subjected to Western blot are shown in the lowest panels. (D) Interaction between endogenous TEAD4 and p-Smad3 was examined using TGF-β–treated Y-MESO-27 cells. (E) Y-MESO-27 cells were infected with a TEAD4 lentiviral vector. After 4 d, the cells were treated with TGF-β, and lysates were immunoprecipitated with Smad2/3 antibodies and detected by YAP antibodies. (F) NCI-H290 cells were transfected with the *CTGF*-luciferase reporter plasmid and combinations of TGF-β, YAP, and p300. Results are expressed as mean ± SEM and are representative of three independent assays. (G) NCI-H290 cells were transfected with the *CTGF*-luciferase reporter together with the indicated plasmids. Luciferase activity (top) and protein levels (bottom) are shown. Results are expressed as mean ± SEM and are representative of three independent assays. (H) ChIP analysis was performed using MSTO-211H cells by pulling down endogenous Smad2/3, p300, YAP, and TEAD4. *CTGF* promoter with Smad- and TEAD-binding adjacent regions was amplified by PCR. The value was normalized by input. The results shown are representative of three independent assays. (I) ChIP-reChIP assay was performed using TGF-β–treated MSTO-211H cell lysates, followed by quantitative PCR (qPCR). The first and second primary antibodies used for immunoprecipitation are indicated. (H and I) Results are expressed as mean ± SEM and are representative of three independent assays.

formation to further demonstrate both binding and functional activity.

Transient transfection experiments with HEK293 cells revealed that Smad3, p300, and YAP coprecipitate with both TEAD3 and TEAD4, although binding affinity was much stronger for TEAD4, compared with TEAD3 (Fig. 4, A and B). An immunoprecipitation assay using HEK293T cells with ectopic expression of Smad3 and p300 showed that the binding between ectopic p300 and endogenous YAP was enhanced in the presence of ectopic Smad3 (Fig. 4 C, second panel). The interaction of endogenous YAP with ectopic Smad3 was enhanced in the presence of ectopic p300 (Fig. 4 C, third panel), and on the contrary, the binding of ectopic p300 to endogenous YAP was much stronger in the presence of Smad3 (Fig. 4 C, fourth panel). Furthermore, endogenous TEAD4 bound to ectopic p300 in the presence of ectopic Smad3 and with ectopic Smad3 in the presence of ectopic p300 (Fig. 4 C, fifth and sixth panels). Using Y-MESO-27 cells, an MM cell line in which *LATS2* has been deleted (Murakami et al., 2011), we confirmed the endogenous interactions between TEAD4 and phosphorylated Smad3. TGF-β treatment further increased the amount of p-Smad3 that was immunoprecipitated with TEAD4 (Fig. 4 D). Consistent with the aforementioned results, interaction between endogenous Smad2/3 and YAP was observed under the existence of TEAD4 protein in Y-MESO-27 cells (Fig. 4 E). We also examined whether Smad3 and p300 augment YAP–TEAD4 complex formation and found that neither Smad3 nor p300 affects the interaction between YAP and TEAD4 (unpublished data). These data suggest that YAP, Smad3, p300, and TEAD4 mutually assist each other to strengthen the formation of a complex based on the stable binding between YAP and TEAD4 on the *CTGF* promoter.

Maximum transcriptional activation of *CTGF* promoter was observed when two proteins were overexpressed under TGF-β treatment (Fig. 4 F). Transfection of TEAD4 instead of YAP did not enhance the transactivation (unpublished data), suggesting that YAP is a prerequisite for YAP–TEAD4–Smad3–p300 complex formation and CTGF activation. We then assessed the significance of the YAP–Smad3 association in this complex. YAP-ΔCC enhanced the transactivation of the *CTGF* promoter to the same extent of full-length YAP, whereas YAP-ΔWW substantially reduced this activity, indicating that YAP–Smad3 binding plays a functionally important role in this complex (Fig. 4 G). Consistent with the presented results, the chromatin immunoprecipitation (ChIP) assay of *CTGF* promoter demonstrates that TGF-β stimulates the binding of endogenous Smad2/3 and p300 to the *CTGF* promoter but not the binding of YAP and TEAD4, which perhaps constitutively reside on the promoter region in MSTO-211H cells (Fig. 4 H). Furthermore, ChIP-reChIP assay using TGF-β–treated MSTO-211H cells showed that YAP, Smad2/3, and TEAD4 reside on the same *CTGF* promoter site (Fig. 4 I). Collectively, these data demonstrate that YAP–TEAD4–Smad3–p300 complex formation on the *CTGF* promoter is crucial for *CTGF* gene expression in MM cells.

CTGF regulates proliferation and ECM production in MM cells in vitro

Given the synergistic activation of the *CTGF* gene by both the Hippo pathway and TGF-β signaling in MM cells, we investigated whether CTGF is essential for the oncogenic properties of these cells. Using an shRNA lentiviral vector system, we examined whether CTGF is required for cell growth in NCI-H290 cells. Knockdown of CTGF suppressed NCI-H290 cell growth to a mean of 77.2% (ShCTGF#1) and 84% (ShCTGF#2), respectively, compared with the growth of the nontarget control (Fig. 5 A). We examined whether the expression of CTGF could modulate foci formation in NCI-H290 cells. Interestingly, CTGF expression showed the same response as the constitutive activation of the TGF-β type I receptor, which showed aggressive formation of foci, whereas the knockdown of CTGF reduced the number of foci (Fig. 5 B). Furthermore, the soft agar colony formation assay showed a reduction in size (Fig. 5 C, left) and the number of colonies in CTGF–knocked down NCI-H290 cells (Fig. 5 C, right). We then assessed whether CTGF expression affects the level of ECM proteins.

There is a study that shows the CTGF protein involvement in attenuation of fibronectin and Collagen 1 production induced by TGF-β in cultured human peritoneal mesothelial cells (Xiao et al., 2010). To confirm whether this CTGF function was also observed in MM cells, we used NCI-H290 cells and found that the CTGF expression affected the mRNA level of *fibronectin* and *COL1A1* in 24 h. As shown in Fig. 2, these two genes were late response genes to TGF-β, showing that CTGF modulates the expression level of ECM proteins as a consequence of a series of signaling (Fig. 5 D). The knockdown of CTGF expression abolished the aggressive formation of foci induced by the constitutively activated TGF-β type I receptor (Fig. 5 E).

CTGF is an important modulator of MM cell growth and deposition of ECM

Immunohistochemical analysis using nine human MM cells implanted into the thoracic cavity of nude mice again showed clear nuclear staining of p-Smad2, with little staining in stromal or normal tissues (Fig. 6 A, left). Nuclear staining of YAP was also observed in most tissues, although staining varied widely from weak to strong and showed a moderate correlation with the cytoplasmic staining of CTGF in MM cells (Fig. 6 A, right). Of note, the amount of stroma, which plays an important role in the cancer microenvironment, also appeared to strongly correlate with CTGF expression in MMs, suggesting that CTGF regulates the growth of MMs and also leads to a tumor environment suitable for their growth.

Based on the aforementioned findings implicating TGF-β signaling and CTGF in MM cell and tumor growth, we determined whether inhibition of TGF-β type I receptor signaling and CTGF expression induces growth suppression of MM tumors in a mouse model. SD-208 is an orally bioactive TGF-β type I receptor kinase inhibitor previously shown to significantly reduce osteolytic lesions in breast cancer bone

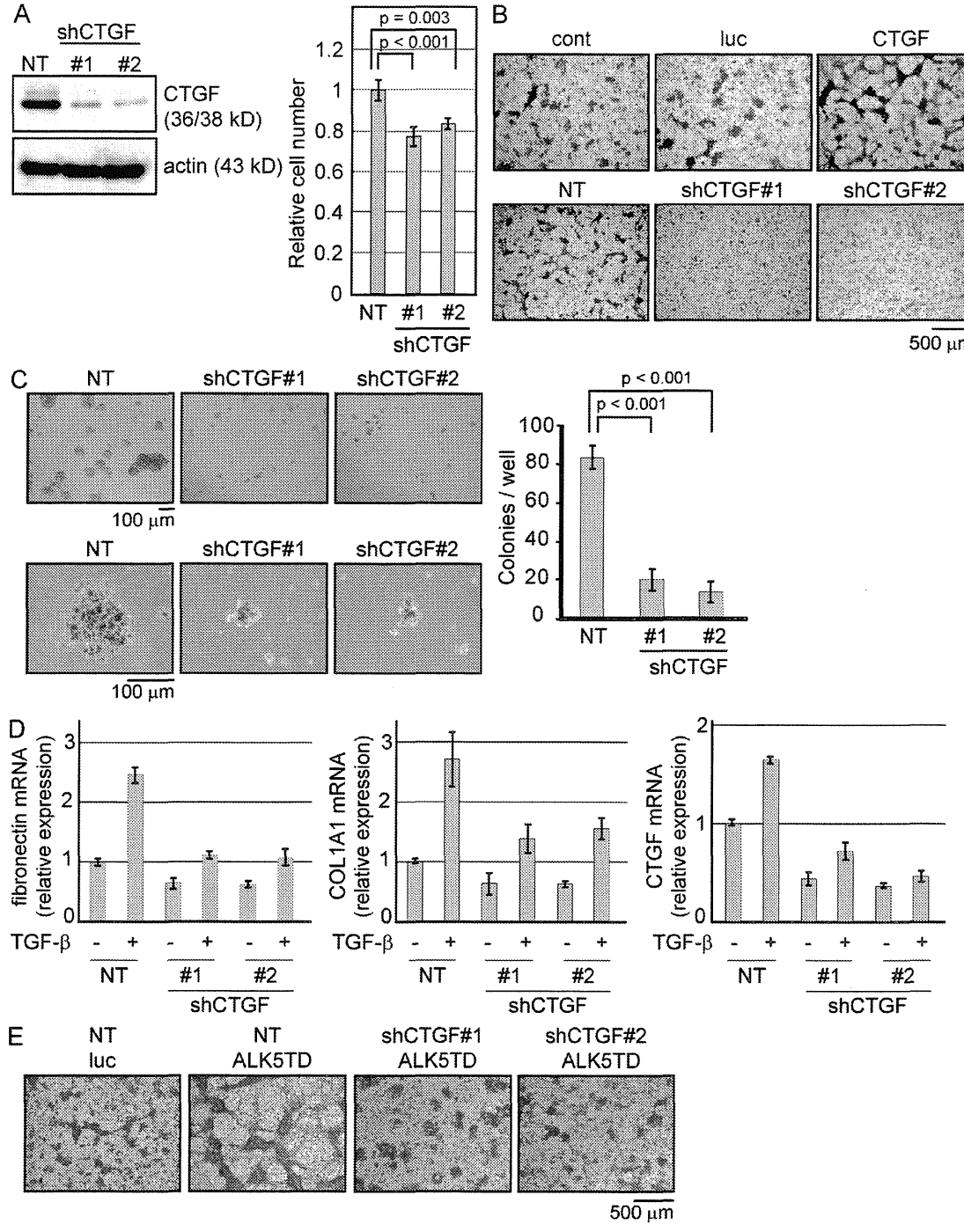

Figure 5. CTGF expression affects the growth and malignancy of MM cells. (A) NCI-H290 cells were lentivirally infected with shRNA against CTGF (shCTGF). Cell proliferation analysis was performed 4 d after lentiviral shRNA transduction. The endogenous protein level of CTGF was confirmed by Western blotting (left). Cell number was counted and normalized to the nontarget (NT) control (right). (B) NCI-H290 cells were infected with the indicated lentivirus expression vectors and stained with Giemsa after 14 d. HA-tagged luciferase (luc) was used as a control for CTGF and nontarget control for shCTGF. The results shown are representative of three independent assays. (C) Soft agar colony formation assay was performed using shRNA lentivirus–transduced NCI-H290 cells and stained with 0.5 mg/ml p-iodonitrotetrazolium after 10 d. The lower panel shows the mean size of colonies in each well. Colony number was counted in a range with a >100-μm diameter. (D) Real-time RT-PCR was performed using NCI-H290 cells infected by shRNA lentivirus 24 h after the treatment of TGF-β. (A, C, and D) Results are expressed as mean ± SEM and are representative of three independent assays. (E) NCI-H290 cells infected with the shCTGF lentivirus were kept under puromycin selection. Cells were then infected with the ALK5 lentivirus and stained using Giemsa after 14 d. The results shown are representative of three independent assays.

metastasis (Dunn et al., 2009). Oral gavage with 60 mg/kg SD-208 decreased the p-Smad2 level in NCI-H290 tissues implanted in the thoracic cavities of nude mice and further prolonged their survival (Fig. 6 B). Knockdown of CTGF expression in NCI-H290 cells also facilitated longer survival of mice (Fig. 6 C). These data demonstrate that the blockade of TGF-β signaling and suppression of CTGF protein expression impair MM tumor growth.

To further examine the contribution of CTGF expression in MM tumor growth, immunohistochemical staining was again performed by staining the 24 tissue specimens used earlier (Fig. 1 A) with YAP and CTGF antibodies. Although p-Smad2 nuclear staining was observed in all MM tumor tissues, strong CTGF expression in the cytoplasm of MM cells was dominantly observed in sarcomatoid tumors but was weak in epithelioid tumors and normal mesothelial cells (Fig. 6 D and Table 2). YAP nuclear staining was also observed in sarcomatoid tumors but was not dominant in epithelioid and normal cells, although there was a strong staining in cytoplasm in epithelioid tumor cells (Fig. 6 E and Table 2). Sporadic nuclear staining of YAP was observed in reactive mesothelioma, but compatible with the previous study which shows the amplification of *YAP* oncogene (Yokoyama et al., 2008). YAP staining in mesothelioma tissues was much stronger than normal tissues. 7 out of 12 epithelioid tissues were positively stained for YAP, suggesting that some additional factor that is present in sarcomatoid tumors might be required for CTGF expression.

Sarcomatoid mesotheliomas are composed of spindle cells with abundant stroma that resemble the histological appearance of Y-MESO-27 and NCI-H2052 cells implanted in mice (Figs. 1 A and 6 A). In MM tumor patients, histological subtype is one of the most important predictors of survival and in the selection of appropriate treatment. Our findings revealed a strong association between MM cell growth and TGF-β signaling, partially through synergistic enhancement of CTGF expression with YAP. Furthermore, we identified the involvement of CTGF in subsequent induction of stroma in MM tumors and its possible association with malignancy. Based on these findings, TGF-β and CTGF are strong candidates for targeting therapies that may be effective for both MM cells and the surrounding stroma.

DISCUSSION

MM is a cancer that often shows dissemination and progression in the thoracic or peritoneal cavity at diagnosis, and many problems remain unresolved regarding its early diagnosis and effective treatment. MM shows resistance to conventional chemotherapies probably because it does not originate from the epithelial cells and does not have the same characteristics as these cells, which can be treated with drugs. Although patients with MM usually have a poor clinical prognosis, both basic and clinical studies are lacking compared with the studies on other malignancies. Thus, there is an urgent need to develop new therapies. Based on a previous study concerning TGF-β secretion from MMs into pleural fluid and the sensitivity of murine mesothelioma to TGF-β type I receptor kinase inhibitor (Suzuki et al., 2007), we speculated a strong association between MM growth and TGF-β signaling. Moreover, MM is usually accompanied by a thick fibrotic layer that may cause thickening of the pleura and subsequent functional disorder of the lung. Because TGF-β is known to contribute to fibrosis through the Smad3-dependent pathway (Roberts et al., 2006), this fibrotic change in MM tissues could also be primarily induced by TGF-β activation. If TGF-β was continuously produced by MM tumors, TGF-β might further affect the surrounding cancer environment including fibrosis, vascularization, and suppression of immune responses. In our study, TGF-β treatment could successfully activate the Smad2/3 pathway in both normal MeT-5A and malignant MM cells, suggesting that TGF-β signaling is intact during the progression of malignancy.

One of the major categories of the TGF-β–responsive genes commonly up-regulated in both MeT-5A and Y-MESO-27 cells were ECM-related proteins that may provide anchorage for cells, making malignant cancer cells more aggressive (Radisky and Radisky, 2007; Levental et al., 2009). Furthermore, p-Smad2 nuclear staining was observed in all human MM tissue specimens, regardless of histological subtype, and also in reactivated normal mesothelial cells in MM patients, which may be evidence that constitutive activation of TGF-β signaling is a common feature during tumor development. Blockade of the TGF-β pathway in MM cells resulted in growth suppression both in vitro and in vivo. These data strongly support the hypothesis that TGF-β–stimulated growth is an innate property of mesothelial cells, which is conserved during the progression of malignancy.

Because at least 75% of MM tumors have a disturbance in the Hippo signaling pathway, this type of tumor mostly relies on this pathway for oncogenesis, whereas only 20–25% of MM tumors have a p53 mutation, which is the most frequently inactivated tumor suppressor gene in human malignancies (Sekido, 2010). Although many types of cancer cells have been recently reported to exhibit a disturbance in the Hippo signaling pathway, MM tumors have an extremely high frequency of disturbance in this pathway, indicating that the Hippo signaling pathway is the main tumor suppressor in these cells. Therefore, we investigated a possible functional link between the TGF-β and Hippo signaling pathways in mesothelioma genesis. Determining the cross talk between distinct pathways is important when searching for suitable targets of molecular target therapies because a blockade in one pathway might be insufficient to obtain the maximum effect. If there are some strong growth-driving target genes that overlap the two distinct pathways, these genes could play an important role in mesothelioma cells.

A previous study has shown that TAZ/YAP regulates the localization of Smad2/3 in response to cell density during embryogenesis (Varelas et al., 2008). TAZ/YAP dephosphorylation drives the nuclear accumulation of TAZ/YAP and Smad2/3 in the nucleus. Our data show that the two pathways also converge to regulate the transcription of disease-related target genes in MM and further relate to promote malignancy.

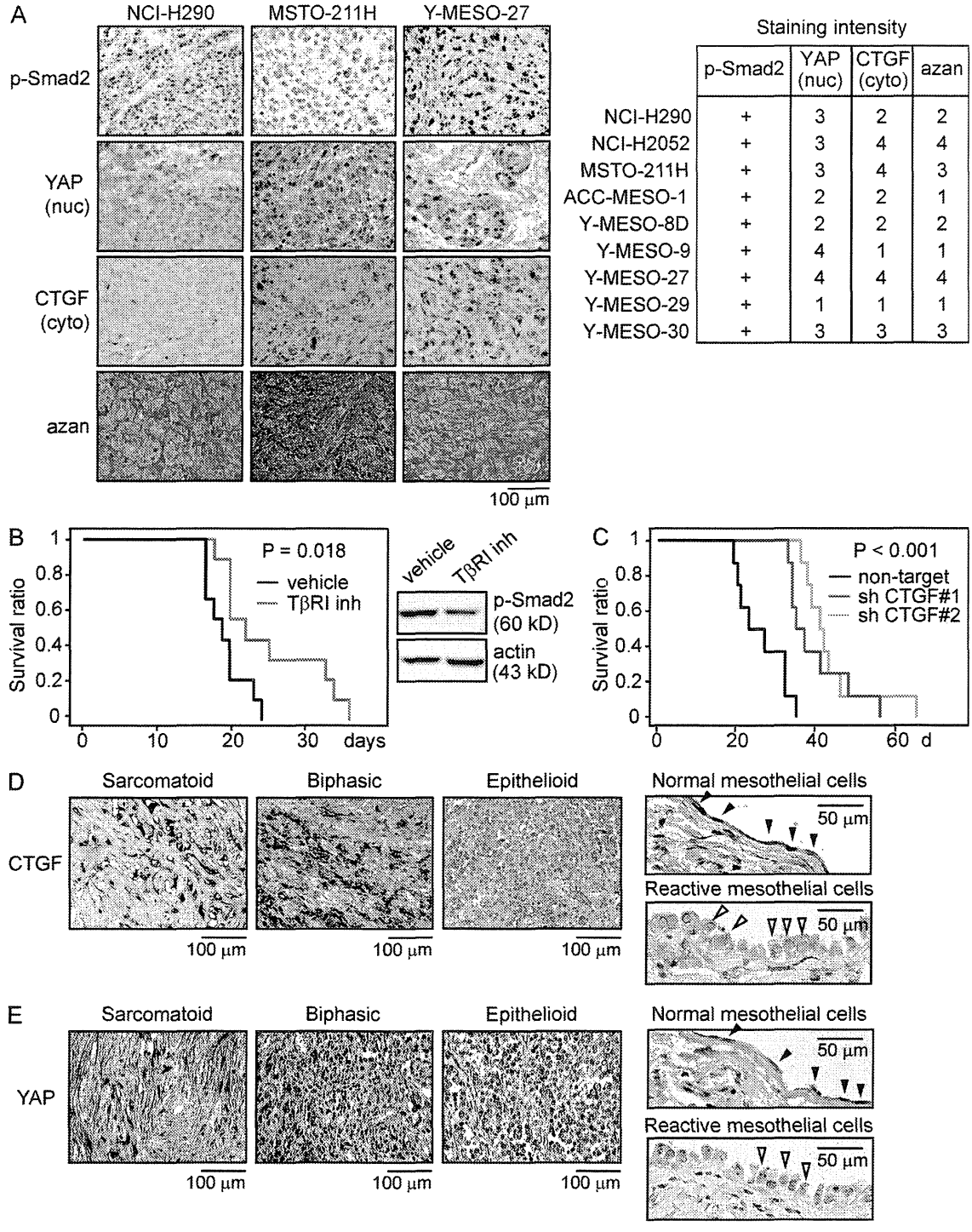

Figure 6. CTGF expression associates with the deposition of ECM protein in MM tumors. (A) Immunohistochemical staining of MM cells implanted in the thoracic cavities of athymic nude mice using p-Smad2, YAP, and CTGF antibodies. Collagen fibers were visualized in blue by azan staining (left). The right panel shows the scoring of the immunohistochemical staining. Staining intensity was scored as follows: 1, normal; 2, mild; 3, moderate; and 4, severe. (B) The Kaplan-Meier method was used to monitor the survival of athymic nude mice after the thoracic implantation of the NCI-H290 cells, followed by initiation of treatment with the TβRI inhibitor SD-208 (60 mg/kg) 2 d later (left). SD-208 was administered daily by oral gavage for 10 d ($n = 9$), and then tumor tissues were excised and subjected to Western blotting (right). The results shown are representative of two independent experiments. (C) NCI-H290 cells lentivirally transduced with shRNA constructs were implanted into the thoracic cavities of athymic nude mice, and survival was monitored ($n = 8$). The results shown are representative of three independent experiments. (D and E) Immunohistochemical staining of CTGF and YAP in MM tissues derived from patients with sarcomatoid as well as biphasic and epithelioid subtypes. Normal mesothelial cells (closed arrowheads) and reactivated normal mesothelial cells (open arrowheads) are shown in the right panels.

Table 2. CTGF expression in MM cells was dominantly observed in sarcomatoid type tissues

No.	Pathological subtype	Features	p-Smad2 (nuclear)	YAP (nuclear)	CTGF (cytoplasm)
1	Sarcomatoid	Fibrous	+	+	+
2	Sarcomatoid	Fibrous	+	+	+
3	Sarcomatoid	Fibrous	+	+	+
4	Sarcomatoid	Fibrous	+	±	+
5	Sarcomatoid	Fibrous	+	±	+
6	Sarcomatoid	Fibrous	+	+	+
7	Sarcomatoid	Fibrous	+	±	+
8	Desmoplastic (sarcomatoid)	Fibrous	+	+	+
9	Desmoplastic (sarcomatoid)	Fibrous	+	+	+
10	Biphasic	Fibrous sarcomatoid, tubulopapillary	+	S: +, E: ±	S: +, E: −
11	Biphasic	Fibrous sarcomatoid, microcystic	+	S: ±, E: ±	S: +, E: +
12	Biphasic	Fibrous sarcomatoid, solid (well-differentiated)	+	S: +, E: +	S: ±, E: ±
13	Epithelioid	Fibrous microcystic	+	+	+
14	Epithelioid	Tubulopapillary	+	−	−
15	Epithelioid	Microcystic, tubulopapillary	+	+	±
16	Epithelioid	Tubulopapillary	+	−	−
17	Epithelioid	Tubulopapillary	+	−	−
18	Epithelioid	Tubulopapillary	+	−	−
19	Epithelioid	Tubulopapillary	+	−	−
20	Epithelioid	Microcystic	+	+	−
21	Epithelioid	Tubulopapillary	+	+	−
22	Epithelioid	Tubulopapillary	+	+	±
23	Epithelioid	Solid (well-differentiated)	+	+	−
24	Epithelioid	Tubulopapillary	+	+	−

Immunohistochemical staining of 24 patients was performed using p-Smad2, YAP, and CTGF antibodies. Tissues were classified based on pathological subtypes. +, positive; ±, partially positive; −, negative; S, sarcomatoid part; E, epithelioid part.

Expression of CTGF was controlled by the presence of the YAP–TEAD4–Smad3–p300 complex in the nucleus of the MM, which we identify as a novel therapeutic target in MM.

Consistent with previous data showing that inactivation of the *NF2* and Hippo pathway is the most frequent defect in mesothelioma, immunohistochemical analysis of MM specimens revealed overexpression and nuclear accumulation of YAP, whereas no signals were observed in normal pleural mesothelial cells (Yokoyama et al., 2008). Nuclear accumulation of YAP is responsible for MM cells undergoing oncogenic events, and normal mesothelial cells might have less YAP-dependent growth because of down-regulation by the intact Hippo pathway.

In looking for synergy between the inactivation of the Hippo pathway and TGF-β signaling, we found that knocking down YAP, which predominantly resides in the nucleus of NCI-H290 cells, affected only a small portion of TGF-β–responsive genes, suggesting that functional association between YAP and Smad2/3 only occurs under a specific situation. *CTGF* is a gene carrying both a TEAD-binding site and a consensus Smad-binding site adjacent to each other on its promoter. Although the binding between YAP and Smad3 is not overly strong, it results in an obvious synergistic activation in the reporter assay or CTGF protein expression assay. Even in the immunoprecipitation assay using HEK293 cells, the exogenous overexpression of Smad3 showed weak binding between YAP and Smad3, and we could not detect endogenous binding in mesothelioma cells. This suggests that other components may be responsible for strengthening the YAP–Smad3 binding and promoting transactivation. We found that p300 and TEAD4 are components of the Smad complex, and Smad3 preferentially binds to TEAD4 rather than to YAP. This hypothesis enabled us to determine not only the physical interactions but also the functional meanings of Smad3–TEAD4 and Smad3–YAP bindings at the endogenous level.

CTGF is a 36/38-kD cysteine-rich protein whose expression is often observed in stroma, which might reflect an active tumor–stromal interaction (Wahab and Mason, 2006). Enhancement of tumor–stromal interactions can potentially promote cancer cell invasion and metastasis. In addition to recent studies that indicate that tumor cell–derived CTGF plays an important role in the proliferation of breast cancer cells (Zhao et al., 2008) and growth of pancreatic tumors (Bennewith et al., 2009), CTGF also affects vascularization, migration, and epithelial-mesenchymal transition in the context of oncogenic properties (Wahab and Mason, 2006). Our immunohistochemical staining of MM cells implanted in the thoracic cavities of nude mice revealed that p-Smad2 constantly resided in the nucleus, whereas the level of YAP in

the nucleus varied among cells. CTGF expression was moderately correlated to YAP localization in the nucleus, consistent with our result that maximum CTGF expression was achieved by activation of TGF-β signaling and inactivation of the *NF2* tumor suppressor pathway. The high levels of YAP nuclear staining and low levels of CTGF staining seen in Y-MESO-9 cells and in some epithelioid type human MM tissues were the exception to this relationship, suggesting that there might be additional undiscovered mechanisms participating in the regulation and of CTGF expression.

Importantly, there was a strong association between MM CTGF expression and the amount of stroma surrounding MM cells. As noted in Y-MESO-29 cells, the cells that grew in solid/nodular form with thin connective tissues surrounding the mass of tumor cells tended to express rather low levels of CTGF. In contrast, NCI-H2052 and Y-MESO-27 cells, which have high levels of CTGF staining, showed extensive accumulation of collagen fibers. Approximately 60% of MM tumors show histologically epithelioid subtype, whereas sarcomatoid and biphasic types each account for 20% (Flores et al., 2007). From our findings which showed that sarcomatoid type MM tumors exhibit strong CTGF staining, we speculate that tumor-derived CTGF has a strong correlation with the deposition of surrounding connective tissue in MM tumors, further linking CTGF to MM malignancy. Our data suggest that TGF-β signaling is active in both the normal and transformed mesothelium. However, in the transformed mesothelium, the activation of the Hippo pathway synergizes with the TGF-β pathway signaling to increase CTGF production and thereby amplify the profibrotic and colony-stimulating effects of TGF-β and potentially inducing other protumorigenic effects in the microenvironment.

Determining the proper way to target CTGF expression is critical for clinical applications. To directly target CTGF, one must first decide whether to use antibody or antisense therapies. Our data also suggest that there might be additional undiscovered mechanisms that participate in the regulation of CTGF expression. Furthermore, the mechanism that allows CTGF to exert its effects has not yet been clarified. Further research regarding CTGF expression and its functions might lead to the discovery of new targets that could be used to regulate CTGF expression. The number of available targets could be increased if TGF-β and Hippo signaling pathways were included. There are some studies indicating that systemic administration of TGF-β antagonists can suppress the growth of mesotheliomas primarily through the reactivation of antitumor immune responses (Suzuki et al., 2004, 2007). In this study, we demonstrated that these antagonists have an important mechanistic contribution to the tumor parenchyma as well. The TGF-β type I receptor inhibitor or TGF-β antibody might be suitable for suppressing the activation of the TGF-β pathway and further attenuate CTGF expression in MM. Regarding the Hippo signaling pathway, drugs that inhibit YAP translocation into the nucleus or activate Hippo signaling are expected to be developed. Simultaneous suppression of both the TGF-β and Hippo signaling pathways may considerably reduce CTGF expression. Our findings propose Smad3 and YAP to be the factors influencing expression of CTGF, and we show for the first time that CTGF might be a strong candidate for molecularly targeted therapy, affecting both mesothelioma cell growth and the tumor microenvironment.

MATERIALS AND METHODS

Cell culture and reagents. HEK293 cells were grown in Dulbecco's Modified Eagle's Medium (Invitrogen) supplemented with 10% FBS. MeT-5A, NCI-H2052, and MSTO-211H cells were purchased from the American Type Culture Collection. NCI-H290 cells were gifts from A.F. Gazdar (University of Texas Southwestern Medical Center, Dallas, TX). ACC-MESO-1, Y-MESO-8D, 9, 14, 27, 29, and 30 cells were established in our laboratory, as reported previously (Taniguchi et al., 2007). All MM cell lines were cultured in RPMI 1640 (Invitrogen) supplemented with 10% FBS. Human recombinant TGF-β1 was purchased from R&D Systems. SD-208 (2,4-disubstituted pteridine; an ATP-competitive inhibitor of TGF-β RI kinase) was purchased from Sigma-Aldrich or synthesized by Epichem Pty Ltd. and dissolved in DMSO as 10-μM stocks or at 7.5 mg/ml with 0.5% (wt/vol) methylcellulose.

Soft agar colony formation assay. The soft agar colony formation assay was performed using standard techniques. MeT-5A cells were trypsinized, and 2×10^4 cells were plated in 0.3% top agarose and cultured for 7 d.

Western blot and immunoprecipitation analysis. Cells were washed with ice-cold PBS, lysed on ice for 30 min in lysis buffer (10 mM Hepes, 200 mM NaCl, 30 mM sodium pyrophosphate, 50 mM NaF, 5 μM $ZnCl_2$, and 1.0% Triton X-100, pH 7.5) supplemented with protease inhibitor cocktail (Roche), and centrifuged at 12,000 *g* for 20 min. Supernatants were immunoprecipitated with Immunoprecipitation kit–Dynabeads Protein G (Invitrogen) according to the manufacturer's instructions, using anti-YAP (63.7; Santa Cruz Biotechnology, Inc.), p300 (C-20; Santa Cruz Biotechnology, Inc.), TEAD4 (aa 151–260; Abnova), Smad2/3 (BD and Cell Signaling Technology), HA (Y-11; Santa Cruz Biotechnology, Inc.), or FLAG (M2; Sigma-Aldrich) antibody. Immunoprecipitated proteins were resolved by 10% Tris-glycine SDS-PAGE (Invitrogen), transferred to Immobilon-P membranes (Millipore), and detected with the appropriate primary antibody. Western blots were prepared by standard procedures using anti–p-Smad2/3 (Cell Signaling Technology), YAP1 (EP1674Y; Abcam), CTGF (L-20; Santa Cruz Biotechnology, Inc.), actin monoclonal (Millipore), and other antibodies described above. Immunoreactivity was detected by ECL (GE Healthcare).

Transcriptional reporter assays. Luciferase assays were performed using the Dual-Luciferase Reporter Assay System (Promega) in which Renilla luciferase plasmids were cotransfected as a control to standardize the transfection efficiency. All activity results are normalized to Renilla expression and are representative of three independent assays.

RNA interference vectors in human MM cells. To generate lentivirus that transcribes shRNA, short hairpin oligonucleotides were inserted into pLentiLox 3.7 containing the U6 promoter and PLKO.1 (Sigma-Aldrich) and transfected into HEK293FT cells together with VSVG, RSV-REV, and pMDLg/pRRE. Short hairpin oligonucleotides for YAP (Yokoyama et al., 2008) and CTGF (Zhao et al., 2008) were designed as described previously. A plasmid vector containing the U6 promoter and puromycin-resistance gene was used for transient expression of shYAP (Yokoyama et al., 2008).

Expression profiling with microarrays. Extracted mRNA was subjected to generate cRNA, which was labeled with Cy3 or Cy5 (GE Healthcare) using a low RNA Fluorescent Linear Amplification kit (Agilent Technologies) according to the manufacturer's protocol. Labeled cRNA was then hybridized to an Agilent 44K Whole Human Genome Microarray, followed by confocal laser scanning (Agilent Technologies). The microarray data have been deposited in ArrayExpress under accession no. E-TABM-1144.

Real-time RT-PCR. Quantitative real-time RT-PCR was performed using first-strand complementary DNA with the TaqMan Universal PCR Master Mix (Applied Biosystems), and amplification was performed with an ABI 7500 Real-time PCR System (Applied Biosystems) according to the manufacturer's instructions. Quantification of GAPDH transcripts as an internal control for the amount and quality of cDNA was performed for all samples.

ChIP. The ChIP assay was performed using the ChIP-IT Express Magnetic Chromatin Immunoprecipitation kit (Active Motif) according to the manufacturer's instructions, followed by real-time RT-PCR with the forward primer 5′-ATATGAATCAGGAGTGGTGCGA-3′ and reverse primer 5′-CAACTCACACCGGATTGATCC-3′. The antibodies used were anti-YAP (H-125; Santa Cruz Biotechnology, Inc.), p300 (C-20; Santa Cruz Biotechnology, Inc.), and Smad2/3 (BD). Re-ChIP-IT Magnetic Chromatin Re-Immunoprecipitation kit (Active Motif) was used for the ChIP-reChIP experiment.

Animal experiments. 7–8-wk-old female athymic nude mice of KSN strain (Shizuoka Laboratory Animal Center) were weighed and randomly assigned to different treatment groups. Lentivirally infected or uninfected NCI-H290 cells were then orthotopically injected into the right thoracic cavity of each mouse. To examine the effect of TGF-β type I receptor kinase inhibition, mice (n = 8) were daily treated with single 0.2-ml doses of 0.5% (wt/vol) methylcellulose as a vehicle or 60 mg/kg SD-208 by oral gavage as described previously (Uhl et al., 2004) for 10 d, starting 2 d after tumor cell inoculation. The experimental design was approved by the Animal Care Committee of the Aichi Cancer Center Research Institute, and the animals were cared for in accordance with institutional guidelines as well as the Guidelines for Proper Conduct of Animal Experiments (Science Council of Japan, June 1, 2006).

Immunohistochemistry. The tumor-bearing mice were sacrificed under deep anesthesia and excised the intrathoracic tumor tissue, which was fixed in 10% neutral-buffered formalin and processed for histopathological (hematoxylin and eosin and azan staining) and immunohistochemical examination using an indirect immunoperoxidase method. The antibodies used for immunohistochemical staining were anti–p-Smad2, p-specific (Ser 463/467; Millipore), YAP (H-125; Santa Cruz Biotechnology, Inc.), and CTGF (L-20; Santa Cruz Biotechnology, Inc.).

Statistical analysis. Survival period was analyzed by the Kaplan-Meier method and compared using the log-rank test. All reported p-values were two-sided, with $P < 0.05$ considered statistically significant. Calculations were performed with StatView software version 5.0 (Abacus Concepts).

Online supplemental material. Fig. S1 shows that TGF-β affects the signaling of MM cells. Online supplemental material is available at http://www.jem.org/cgi/content/full/jem.20111653/DC1.

We thank L.M. Wakefield and A. Hata for comments on the manuscript and K.C. Flanders, K. Kawaguchi, T. Mizuno, F. Ishiguro, K. Shinjo, and T. Matsuki for useful discussions. We thank M. Kizuki, N. Saito, and M. Tsuji for excellent technical assistance.

This work was supported by funds from the 24th General Assembly of the Japanese Association of Medical Sciences (to M. Fujii), funds from the Aichi Cancer Research Foundation (to M. Fujii), and Grants-in-Aid for Scientific Research from the Japan Society for the Promotion of Science (20590420 and 23592788 to M. Fujii) and partly by a Special Coordination Fund for Promoting Science and Technology from the Ministry of Education, Culture, Sports, Science and Technology of Japan (H18-1-3-3-1 to Y. Sekido), Grants-in-Aid for Scientific Research (22300338 to Y. Sekido), Grants-in-aid for Third-Term Comprehensive Control Research for Cancer from the Ministry of Health, Labor and Welfare of Japan (to Y. Sekido), the Takeda Science Foundation (Y. Sekido), and the Kobayashi Foundation for Cancer Research (Y. Sekido).

The authors have no additional financial interests.

Submitted: 8 August 2011
Accepted: 12 January 2012

REFERENCES

Alarcón, C., A.I. Zaromytidou, Q. Xi, S. Gao, J. Yu, S. Fujisawa, A. Barlas, A.N. Miller, K. Manova-Todorova, M.J. Macias, et al. 2009. Nuclear CDKs drive Smad transcriptional activation and turnover in BMP and TGF-β pathways. *Cell.* 139:757–769. http://dx.doi.org/10.1016/j.cell.2009.09.035

Anzano, M.A., A.B. Roberts, J.M. Smith, M.B. Sporn, and J.E. De Larco. 1983. Sarcoma growth factor from conditioned medium of virally transformed cells is composed of both type α and type β transforming growth factors. *Proc. Natl. Acad. Sci. USA.* 80:6264–6268. http://dx.doi.org/10.1073/pnas.80.20.6264

Bennewith, K.L., X. Huang, C.M. Ham, E.E. Graves, J.T. Erler, N. Kambham, J. Feazell, G.P. Yang, A. Koong, and A.J. Giaccia. 2009. The role of tumor cell-derived connective tissue growth factor (CTGF/CCN2) in pancreatic tumor growth. *Cancer Res.* 69:775–784. http://dx.doi.org/10.1158/0008-5472.CAN-08-0987

Bianchi, A.B., S.I. Mitsunaga, J.Q. Cheng, W.M. Klein, S.C. Jhanwar, B. Seizinger, N. Kley, A.J. Klein-Szanto, and J.R. Testa. 1995. High frequency of inactivating mutations in the neurofibromatosis type 2 gene (NF2) in primary malignant mesotheliomas. *Proc. Natl. Acad. Sci. USA.* 92:10854–10858. http://dx.doi.org/10.1073/pnas.92.24.10854

de Larco, J.E., and G.J. Todaro. 1978. Growth factors from murine sarcoma virus-transformed cells. *Proc. Natl. Acad. Sci. USA.* 75:4001–4005. http://dx.doi.org/10.1073/pnas.75.8.4001

Dong, J., G. Feldmann, J. Huang, S. Wu, N. Zhang, S.A. Comerford, M.F. Gayyed, R.A. Anders, A. Maitra, and D. Pan. 2007. Elucidation of a universal size-control mechanism in *Drosophila* and mammals. *Cell.* 130:1120–1133. http://dx.doi.org/10.1016/j.cell.2007.07.019

Dunn, L.K., K.S. Mohammad, P.G. Fournier, C.R. McKenna, H.W. Davis, M. Niewolna, X.H. Peng, J.M. Chirgwin, and T.A. Guise. 2009. Hypoxia and TGF-β drive breast cancer bone metastases through parallel signaling pathways in tumor cells and the bone microenvironment. *PLoS ONE.* 4:e6896. http://dx.doi.org/10.1371/journal.pone.0006896

Flores, R.M., M. Zakowski, E. Venkatraman, L. Krug, K. Rosenzweig, J. Dycoco, C. Lee, C. Yeoh, M. Bains, and V. Rusch. 2007. Prognostic factors in the treatment of malignant pleural mesothelioma at a large tertiary referral center. *J. Thorac. Oncol.* 2:957–965. http://dx.doi.org/10.1097/JTO.0b013e31815608d9

Fujii, M., L.A. Lyakh, C.P. Bracken, J. Fukuoka, M. Hayakawa, T. Tsukiyama, S.J. Soll, M. Harris, S. Rocha, K.C. Roche, et al. 2006. SNIP1 is a candidate modifier of the transcriptional activity of c-Myc on E box-dependent target genes. *Mol. Cell.* 24:771–783. http://dx.doi.org/10.1016/j.molcel.2006.11.006

Gabrielson, E.W., B.I. Gerwin, C.C. Harris, A.B. Roberts, M.B. Sporn, and J.F. Lechner. 1988. Stimulation of DNA synthesis in cultured primary human mesothelial cells by specific growth factors. *FASEB J.* 2:2717–2721.

Gerwin, B.I., J.F. Lechner, R.R. Reddel, A.B. Roberts, K.C. Robbins, E.W. Gabrielson, and C.C. Harris. 1987. Comparison of production of transforming growth factor-β and platelet-derived growth factor by normal human mesothelial cells and mesothelioma cell lines. *Cancer Res.* 47:6180–6184.

Hamaratoglu, F., M. Willecke, M. Kango-Singh, R. Nolo, E. Hyun, C. Tao, H. Jafar-Nejad, and G. Halder. 2006. The tumour-suppressor genes NF2/Merlin and Expanded act through Hippo signalling to regulate cell proliferation and apoptosis. *Nat. Cell Biol.* 8:27–36. http://dx.doi.org/10.1038/ncb1339

Hay, B.A., and M. Guo. 2003. Coupling cell growth, proliferation, and death. Hippo weighs in. *Dev. Cell.* 5:361–363. http://dx.doi.org/10.1016/S1534-5807(03)00270-3

Holmes, A., D.J. Abraham, S. Sa, X. Shiwen, C.M. Black, and A. Leask. 2001. CTGF and SMADs, maintenance of scleroderma phenotype is independent of SMAD signaling. *J. Biol. Chem.* 276:10594–10601. http://dx.doi.org/10.1074/jbc.M010149200

Ke, Y., R.R. Reddel, B.I. Gerwin, H.K. Reddel, A.N. Somers, M.G. McMenamin, M.A. LaVeck, R.A. Stahel, J.F. Lechner, and C.C. Harris. 1989. Establishment of a human in vitro mesothelial cell model system for investigating mechanisms of asbestos-induced mesothelioma. *Am. J. Pathol.* 134:979–991.

Levental, K.R., H. Yu, L. Kass, J.N. Lakins, M. Egeblad, J.T. Erler, S.F. Fong, K. Csiszar, A. Giaccia, W. Weninger, et al. 2009. Matrix crosslinking forces tumor progression by enhancing integrin signaling. *Cell.* 139:891–906. http://dx.doi.org/10.1016/j.cell.2009.10.027

Massagué, J. 2008. TGFbeta in cancer. *Cell.* 134:215–230. http://dx.doi.org/10.1016/j.cell.2008.07.001

Massagué, J., J. Seoane, and D. Wotton. 2005. Smad transcription factors. *Genes Dev.* 19:2783–2810. http://dx.doi.org/10.1101/gad.1350705

Moses, H.L., E.L. Branum, J.A. Proper, and R.A. Robinson. 1981. Transforming growth factor production by chemically transformed cells. *Cancer Res.* 41:2842–2848.

Murakami, H., T. Mizuno, T. Taniguchi, M. Fujii, F. Ishiguro, T. Fukui, S. Akatsuka, Y. Horio, T. Hida, Y. Kondo, et al. 2011. LATS2 is a tumor suppressor gene of malignant mesothelioma. *Cancer Res.* 71:873–883. http://dx.doi.org/10.1158/0008-5472.CAN-10-2164

Murayama, T., K. Takahashi, Y. Natori, and N. Kurumatani. 2006. Estimation of future mortality from pleural malignant mesothelioma in Japan based on an age-cohort model. *Am. J. Ind. Med.* 49:1–7. http://dx.doi.org/10.1002/ajim.20246

Nishihara, A., J.I. Hanai, N. Okamoto, J. Yanagisawa, S. Kato, K. Miyazono, and M. Kawabata. 1998. Role of p300, a transcriptional coactivator, in signalling of TGF-β. *Genes Cells.* 3:613–623. http://dx.doi.org/10.1046/j.1365-2443.1998.00217.x

Radisky, E.S., and D.C. Radisky. 2007. Stromal induction of breast cancer: inflammation and invasion. *Rev. Endocr. Metab. Disord.* 8:279–287. http://dx.doi.org/10.1007/s11154-007-9037-1

Roberts, A.B., and L.M. Wakefield. 2003. The two faces of transforming growth factor β in carcinogenesis. *Proc. Natl. Acad. Sci. USA.* 100:8621–8623. http://dx.doi.org/10.1073/pnas.1633291100

Roberts, A.B., F. Tian, S.D. Byfield, C. Stuelten, A. Ooshima, S. Saika, and K.C. Flanders. 2006. Smad3 is key to TGF-β-mediated epithelial-to-mesenchymal transition, fibrosis, tumor suppression and metastasis. *Cytokine Growth Factor Rev.* 17:19–27. http://dx.doi.org/10.1016/j.cytogfr.2005.09.008

Robinson, B.W., and R.A. Lake. 2005. Advances in malignant mesothelioma. *N. Engl. J. Med.* 353:1591–1603. http://dx.doi.org/10.1056/NEJMra050152

Ryoo, H.D., and H. Steller. 2003. Hippo and its mission for growth control. *Nat. Cell Biol.* 5:853–855. http://dx.doi.org/10.1038/ncb1003-853

Sekido, Y. 2010. Genomic abnormalities and signal transduction dysregulation in malignant mesothelioma cells. *Cancer Sci.* 101:1–6. http://dx.doi.org/10.1111/j.1349-7006.2009.01336.x

Sekido, Y., H.I. Pass, S. Bader, D.J. Mew, M.F. Christman, A.F. Gazdar, and J.D. Minna. 1995. Neurofibromatosis type 2 (NF2) gene is somatically mutated in mesothelioma but not in lung cancer. *Cancer Res.* 55:1227–1231.

Suzuki, E., V. Kapoor, H.K. Cheung, L.E. Ling, P.A. DeLong, L.R. Kaiser, and S.M. Albelda. 2004. Soluble type II transforming growth factor-β receptor inhibits established murine malignant mesothelioma tumor growth by augmenting host antitumor immunity. *Clin. Cancer Res.* 10:5907–5918. http://dx.doi.org/10.1158/1078-0432.CCR-03-0611

Suzuki, E., S. Kim, H.K. Cheung, M.J. Corbley, X. Zhang, L. Sun, F. Shan, J. Singh, W.C. Lee, S.M. Albelda, and L.E. Ling. 2007. A novel small-molecule inhibitor of transforming growth factor β type I receptor kinase (SM16) inhibits murine mesothelioma tumor growth in vivo and prevents tumor recurrence after surgical resection. *Cancer Res.* 67:2351–2359. http://dx.doi.org/10.1158/0008-5472.CAN-06-2389

Taniguchi, T., S. Karnan, T. Fukui, T. Yokoyama, H. Tagawa, K. Yokoi, Y. Ueda, T. Mitsudomi, Y. Horio, T. Hida, et al. 2007. Genomic profiling of malignant pleural mesothelioma with array-based comparative genomic hybridization shows frequent non-random chromosomal alteration regions including JUN amplification on 1p32. *Cancer Sci.* 98:438–446. http://dx.doi.org/10.1111/j.1349-7006.2006.00386.x

Tsao, A.S., I. Wistuba, J.A. Roth, and H.L. Kindler. 2009. Malignant pleural mesothelioma. *J. Clin. Oncol.* 27:2081–2090. http://dx.doi.org/10.1200/JCO.2008.19.8523

Uhl, M., S. Aulwurm, J. Wischhusen, M. Weiler, J.Y. Ma, R. Almirez, R. Mangadu, Y.W. Liu, M. Platten, U. Herrlinger, et al. 2004. SD-208, a novel transforming growth factor β receptor I kinase inhibitor, inhibits growth and invasiveness and enhances immunogenicity of murine and human glioma cells in vitro and in vivo. *Cancer Res.* 64:7954–7961. http://dx.doi.org/10.1158/0008-5472.CAN-04-1013

Varelas, X., R. Sakuma, P. Samavarchi-Tehrani, R. Peerani, B.M. Rao, J. Dembowy, M.B. Yaffe, P.W. Zandstra, and J.L. Wrana. 2008. TAZ controls Smad nucleocytoplasmic shuttling and regulates human embryonic stem-cell self-renewal. *Nat. Cell Biol.* 10:837–848. http://dx.doi.org/10.1038/ncb1748

Varelas, X., P. Samavarchi-Tehrani, M. Narimatsu, A. Weiss, K. Cockburn, B.G. Larsen, J. Rossant, and J.L. Wrana. 2010. The Crumbs complex couples cell density sensing to Hippo-dependent control of the TGF-β-SMAD pathway. *Dev. Cell.* 19:831–844. http://dx.doi.org/10.1016/j.devcel.2010.11.012

Vassilev, A., K.J. Kaneko, H. Shu, Y. Zhao, and M.L. DePamphilis. 2001. TEAD/TEF transcription factors utilize the activation domain of YAP65, a Src/Yes-associated protein localized in the cytoplasm. *Genes Dev.* 15:1229–1241. http://dx.doi.org/10.1101/gad.888601

Wahab, N.A., and R.M. Mason. 2006. A critical look at growth factors and epithelial-to-mesenchymal transition in the adult kidney. Interrelationships between growth factors that regulate EMT in the adult kidney. *Nephron, Exp. Nephrol.* 104:e129–e134. http://dx.doi.org/10.1159/000094963

Wang, K., C. Degerny, M. Xu, and X.J. Yang. 2009. YAP, TAZ, and Yorkie: a conserved family of signal-responsive transcriptional coregulators in animal development and human disease. *Biochem. Cell Biol.* 87:77–91. http://dx.doi.org/10.1139/O08-114

Wu, S., J. Huang, J. Dong, and D. Pan. 2003. hippo encodes a Ste-20 family protein kinase that restricts cell proliferation and promotes apoptosis in conjunction with salvador and warts. *Cell.* 114:445–456. http://dx.doi.org/10.1016/S0092-8674(03)00549-X

Xiao, L., L. Sun, F.Y. Liu, Y.M. Peng, and S.B. Duan. 2010. Connective tissue growth factor knockdown attenuated matrix protein production and vascular endothelial growth factor expression induced by transforming growth factor-β1 in cultured human peritoneal mesothelial cells. *Ther. Apher. Dial.* 14:27–34. http://dx.doi.org/10.1111/j.1744-9987.2009.00701.x

Yang, Y.C., E. Piek, J. Zavadil, D. Liang, D. Xie, J. Heyer, P. Pavlidis, R. Kucherlapati, A.B. Roberts, and E.P. Böttinger. 2003. Hierarchical model of gene regulation by transforming growth factor β. *Proc. Natl. Acad. Sci. USA.* 100:10269–10274. http://dx.doi.org/10.1073/pnas.1834070100

Yokoyama, T., H. Osada, H. Murakami, Y. Tatematsu, T. Taniguchi, Y. Kondo, Y. Yatabe, Y. Hasegawa, K. Shimokata, Y. Horio, et al. 2008. YAP1 is involved in mesothelioma development and negatively regulated by Merlin through phosphorylation. *Carcinogenesis.* 29:2139–2146. http://dx.doi.org/10.1093/carcin/bgn200

Zhang, N., H. Bai, K.K. David, J. Dong, Y. Zheng, J. Cai, M. Giovannini, P. Liu, R.A. Anders, and D. Pan. 2010. The Merlin/NF2 tumor suppressor functions through the YAP oncoprotein to regulate tissue homeostasis in mammals. *Dev. Cell.* 19:27–38. http://dx.doi.org/10.1016/j.devcel.2010.06.015

Zhao, B., X. Ye, J. Yu, L. Li, W. Li, S. Li, J. Yu, J.D. Lin, C.Y. Wang, A.M. Chinnaiyan, et al. 2008. TEAD mediates YAP-dependent gene induction and growth control. *Genes Dev.* 22:1962–1971. http://dx.doi.org/10.1101/gad.1664408

Zhao, B., J. Kim, X. Ye, Z.C. Lai, and K.L. Guan. 2009. Both TEAD-binding and WW domains are required for the growth stimulation and oncogenic transformation activity of yes-associated protein. *Cancer Res.* 69:1089–1098. http://dx.doi.org/10.1158/0008-5472.CAN-08-2997

Oncogene (2012) **31,** 5117-5122

www.nature.com/onc

SHORT COMMUNICATION

YAP induces malignant mesothelioma cell proliferation by upregulating transcription of cell cycle-promoting genes

T Mizuno[1,2], H Murakami[1], M Fujii[1], F Ishiguro[1,2], I Tanaka[1], Y Kondo[1], S Akatsuka[3], S Toyokuni[3], K Yokoi[2], H Osada[1,4] and Y Sekido[1,4]

Malignant mesothelioma (MM) shows frequent inactivation of the *neurofibromatosis type 2* (*NF2*) -tumor-suppressor gene. Recent studies have documented that the Hippo signaling pathway, a downstream cascade of Merlin (a product of *NF2*), has a key role in organ size control and carcinogenesis by regulating cell proliferation and apoptosis. We previously reported that MMs show overexpression of *Yes-associated protein* (YAP) transcriptional coactivator, the main downstream effector of the Hippo signaling pathway, which results from the inactivation of *NF2*, *LATS2* and/or *SAV1 genes* (the latter two encoding core components of the mammalian Hippo pathway) or amplification of *YAP* itself. However, the detailed roles of YAP remain unclear, especially the target genes of YAP that enhance MM cell growth and survival. Here, we demonstrated that YAP-knockdown inhibited cell motility, invasion and anchorage-independent growth as well as cell proliferation of MM cells *in vitro*. We analyzed genes commonly regulated by YAP in three MM cell lines with constitutive YAP-activation, and found that the major subsets of YAP-upregulating genes encode cell cycle regulators. Among them, YAP directly induced the transcription of *CCND1* and *FOXM1*, in cooperation with TEAD transcription factor. We also found that knockdown of *CCND1* and *FOXM1* suppressed MM cell proliferation, although the inhibitory effects were less evident than those of YAP knockdown. These results indicate that constitutive YAP activation in MM cells promotes cell cycle progression giving more aggressive phenotypes to MM cells.

Oncogene (2012) **31,** 5117-5122; doi:10.1038/onc.2012.5; published online 30 January 2012

Keywords: malignant mesothelioma; Hippo pathway; YAP; CCND1; cell cycle

INTRODUCTION

Malignant mesothelioma (MM) is one of the most aggressive neoplasms, which is caused by asbestos exposure.[1,2] It is usually resistant to conventional therapies, and the prognosis of patients is very poor. The median survival of malignant pleural mesothelioma patients after diagnosis is 7-11 months.[1,3,4] There is a 30-40 year interval before clinical presentation of the tumor after asbestos exposure.[5] While the long latency of the disease implies that multiple genetic and epigenetic alterations might be required for MM progression,[6] the detailed molecular pathogenesis of MM has not been well understood.

Among the limited number of genes that are frequently mutated in MMs, inactivation of $p16^{INK4a}/p14^{ARF}$ is detected in over 70% of MMs.[7] The *NF2* gene, which is responsible for the *NF2* familial cancer syndrome, has been shown to be inactivated in 40-50% of MMs.[8,9] A recent study has also indicated that 23% of MM cases had an inactivating mutation of *BAP1*, which encodes a nuclear deubiquitinase.[10,11]

The *NF2* gene encodes Merlin, which is a membrane-cytoskeleton-associated protein with four-point-one, ezrin, radixin and moesin domain, and acts as a tumor suppressor.[12] One of the downstream signaling cascades regulated by Merlin is the Hippo signaling pathway, which is conserved from *Drosophila* to mammalians.[13-15] In MM cells, besides the *NF2* mutation, genetic alterations in the components of the Hippo signaling pathway have also been identified recently, including inactivating mutations of *large tumor suppressor 1* (*LATS1*), *LATS2* and *SAV1*, and amplification of *Yes-associated protein* (*YAP*).[10,16,17] Together with *NF2* mutation, MM shows frequent Merlin-Hippo pathway inactivation, which leads to YAP activation in over 70% of MM cases.[18]

Studies have shown that the Hippo signaling pathway is involved in the cell cycle regulation and the control of organ size.[19,20] The dysregulation of this pathway, which leads to constitutive YAP activation, induces the oncogenic transformation in cooperation with distinct transcription factors such as TEAD family members.[21-24] Overexpression, especially dominant expression in the nuclei compared with the cytoplasm of tumor cells and the oncogenic roles of YAP have been shown in various types of human malignancies.[25-29] On the other hand, the anti-proliferative or apoptosis-inducing function of YAP has also been demonstrated in the context of DNA damage or cellular stress, which induces its binding of YAP with other transcription factors such as p73, a paralog of p53 tumor suppressor.[30-32]

We previously showed that YAP promoted cell proliferation[17] and exogenous LATS2 inhibited cell proliferation via induction of YAP phosphorylation in MM cells.[16] However, the detailed characteristics of YAP oncogenic properties remain unclear, including the exact target genes that are inducible by YAP activation in MM cells. In this study, we aimed to identify the target genes of YAP in MM cells to elaborate how YAP induces the MM-cell malignant phenotypes. We found that cell cycle-regulating genes, including *CCDN1* and *FOXM1*, are induced by YAP, suggesting that the dysregulation of cell cycle regulation is one of the key alterations in which MM cells acquire malignancy by YAP activation.

[1]Division of Molecular Oncology, Aichi Cancer Center Research Institute, Nagoya, Japan; [2]Department of Thoracic Surgery, Nagoya University Graduate School of Medicine, Nagoya, Japan; [3]Department of Pathology and Biological Responses, Nagoya University Graduate School of Medicine, Nagoya, Japan and [4]Department of Cancer Genetics, Program in Function Construction Medicine, Nagoya University Graduate School of Medicine, Nagoya, Japan. Correspondence: Dr Y Sekido, Division of Molecular Oncology, Aichi Cancer Center Research Institute, Kanokoden 1-1, Chikusa-ku, Nagoya, Aichi 464-8681, Japan. E-mail: ysekido@aichi-cc.jp
Received 3 September 2011; revised 19 December 2011; accepted 30 December 2011; published online 30 January 2012

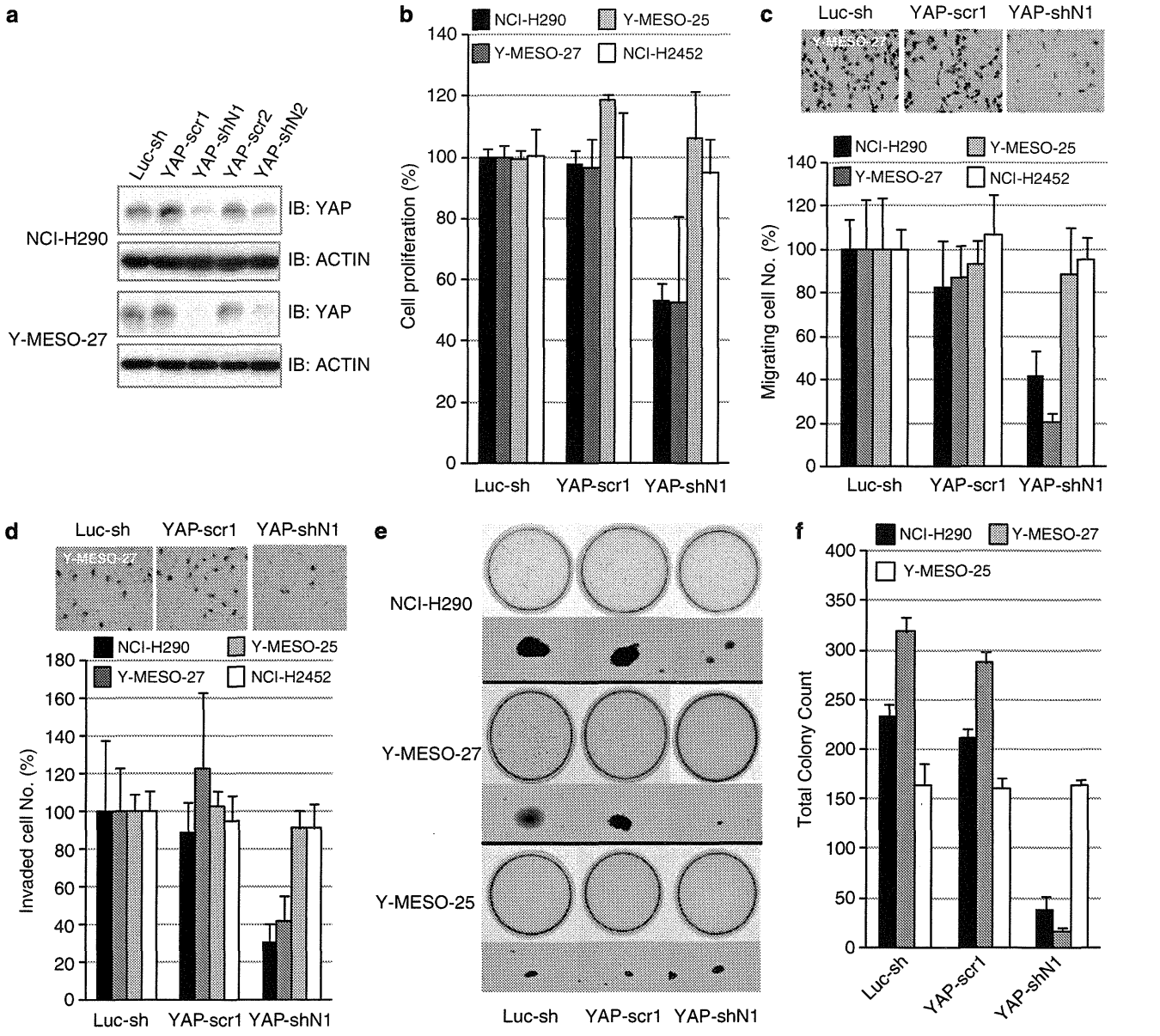

Figure 1. YAP knockdown suppressed malignant phenotypes of MM cell lines with YAP activation (NCI-H290 and Y-MESO-27) but not of those without YAP activation (Y-MESO-25 and NCI-H2452). (**a**) Western blot analyses for knockdown efficacies of short hairpin (sh)-YAP RNA interference lentivirus vectors. Two sh-YAP RNA interference lentivirus vectors (YAP-shN1 and YAP-shN2) contained each target sequence of YAP. Control shRNA vectors for luciferase (Luc-sh) with the target sequence for luciferase and for YAP (YAP-scr1 and YAP-scr2) with each scrambled target sequence were also constructed. Total cell lysates were subjected to western blot analysis using rabbit anti-YAP antibody and mouse anti-β-actin antibody. YAP-shN1 induced more potent YAP suppression compared with YAP-shN2. (**b**) Cell proliferation assay. After 72 h of lentivirus infection, calorimetric assays were performed with Tetra Color One (Seikagaku, Tokyo, Japan) and absorbance was measured at 450 nm. Cell proliferations were reduced to approximately 50% with YAP knockdown in NCI-H290 and Y-MESO-27 cell lines. (**c**) Migration assay. Cell migration and invasion potential were measured by *in vitro* Boyden chamber assays (BD Biosciences Discovery Labware, Bedford, MA, USA). Upper photographs show representative images of the migrating Y-MESO-27 cells. (**d**) Invasion assay. Matrigel matrix insert membrane was used for invasion assay. Upper photographs show representative images of invading Y-MESO-27 cells. (**e**) Soft agar colony formation assays. After a 10 day-incubation, colonies were stained with 0.3% crystal violet. Photographs of low (top) and high magnification (bottom) show that anchorage-independent growth was significantly suppressed with YAP knockdown in NCI-H290 and Y-MESO-27 but not Y-MESO-25 cell line. (**f**) A graphic presentation of the soft agar colony formation assays of (**e**). Columns are the means of experiments, and bars represent s.d. (**b**, **c**, **d**, **f**).

RESULTS AND DISCUSSION

Knockdown of YAP suppressed oncogenic properties of MM cells

We previously reported that several MM cell lines with *NF2* and/or *LATS2* mutations have constitutive YAP activation with low-level phosphorylation of YAP (S127).[16] Using western blot analysis with a panel of 23 MM cell lines, we confirmed that 16 (70%) cell lines showed lower levels of pYAP-S127 than MeT-5A, a transformed normal mesothelial cell line (Supplementary Figure 1). Among them, we selected three MM cell lines with constitutive YAP activation for further analyses; NCI-H290 with *NF2* inactivation, and Y-MESO-27 and Y-MESO-30 with *LATS2* inactivation.

Table 1. Gene ontology and pathway analyses in 228 genes commonly downregulated by YAP knockdown

Rank	*Name*	*Score*	*Score (p)*	*Score (v)*	*Score (c)*
(a) *Top 10 Gene ontology*					
1	Cell cycle (GO:0007049)	137.598	3.791E−042	0.409	0.079
2	Cell cycle process (GO:0022402)	129.250	1.235E−039	0.358	0.090
3	Cell cycle phase (GO:0022403)	117.627	3.897E−036	0.302	0.105
4	Mitotic cell cycle (GO:0000278)	107.258	5.153E−033	0.289	0.097
5	Mitotic phase (GO:0000279)	90.202	7.021E−028	0.214	0.124
6	Regulation of cell cycle (GO:0051726)	86.379	9.939E−027	0.264	0.080
7	Organelle organization (GO:0006996)	82.447	1.517E−025	0.371	0.047
8	Regulation of cell cycle process (GO:0010564)	80.848	4.596E−025	0.176	0.147
9	Regulation of metabolic process (GO:0019222)	76.863	7.275E−024	0.528	0.029
10	Regulation of cellular metabolic process (GO:0031323)	71.798	2.435E−022	0.491	0.030
(b) *Top 10 gene pathway*					
1	Transcriptional regulation by RB/E2F	297.728	2.371E−090	0.234	0.207
2	Transcriptional regulation by FOXM	63.604	7.135E−020	0.043	0.360
3	Aurora signaling pathway	52.246	1.872E−016	0.038	0.258
4	CDK signaling pathway	46.256	1.190E−014	0.043	0.107
5	PLK signaling pathway	45.168	2.531E−014	0.033	0.241
6	Transcriptional regulation by AP-1	35.712	1.777E−011	0.038	0.067
7	Nucleophosmin signaling pathway	29.087	1.753E−009	0.024	0.152
8	Wnt signaling pathway	28.376	2.870E−009	0.029	0.076
9	Transcriptional regulation by Myb	27.041	7.242E−009	0.029	0.065
10	PIN1 signaling pathway	22.329	1.898E−007	0.024	0.061

Abbreviations: AP-1, adaptor-related protein complex 1; CDK, cyclin-dependent kinase; FOXM, forkhead box M; Myb, v-myb myeloblastosis viral oncogene homolog; PIN, peptidylprolyl cis/trans isomerase NIMA-interacting 1; PLK, polo-like kinase; RB/E2F, retinoblastoma/E2F transcription factor.

As we previously showed that YAP inhibition suppressed NCI-H290 cell proliferation,[17] we first confirmed that a newly established YAP-shRNA lentivirus more efficiently suppressed the YAP expression and inhibited the cell proliferation of NCI-H290 cell line and another MM cell line, Y-MESO-27, which had *LATS2* deletion, but not in two other MM cell lines, Y-MESO-25 and NCI-H2452, without YAP activation (Figures 1a and b). Next, we analysed whether YAP knockdown affected other malignant phenotypes of MM cells *in vitro*. Both motility and invasive abilities were significantly inhibited in NCI-H290 and Y-MESO-27 cells (Figures 1c and d). Anchorage-independent growth analysis revealed a nearly complete suppression of colony formation in Y-MESO-27 cells and an 80% decrease in NCI-H290 cells (Figures 1e and f). These results indicate that YAP suppression in MM cells with constitutively activated YAP induces significant suppression of motility, invasion and anchorage-independent growth as well as cell proliferation *in vitro*.

Identification of YAP-regulating genes by microarray-based expression profiling analysis

As for the target genes of YAP orthologs, *cyclin E*, *Diap1* and *bantam* microRNA have been identified for *Drosophila Yokie*.[19] For mammalian YAP, although several genes including the *connective tissue growth factor* (*CTGF*) gene were shown as direct target genes of YAP,[24] other possible candidate target genes for mammalian counterparts do not seem to be really substantiated yet or even excluded, implying that YAP target genes vary among different species as well as among different cell types.

To identify the genes inducible for expression by YAP and responsible for MM cell proliferation, we performed microarray-based expression profiling analysis of the three MM cell lines after YAP knockdown. We found that 1381, 650 and 2097 genes were downregulated to equal or less than 0.5 in the NCI-H290, Y-MESO-27 and Y-MESO-30 cells, respectively, compared with each counterpart cell with the control vector (data not shown). We found that 228 genes were commonly downregulated by YAP knockdown, suggesting that this gene set includes strong candidates for YAP target genes in MM cells (Supplementary Table 1). To characterize the 228 genes, we performed gene ontology analysis and found that the large portion of YAP-regulatory genes is associated with cell cycle regulation (Table 1). Subsequent pathway analysis revealed that the pathways of transcriptional regulation by *RB/E2F* and *FOXM* were most significantly correlated (Table 1).

Meanwhile, our results revealed that 156 genes were commonly upregulated after YAP knockdown over twofold (Supplementary Table 1). Gene ontology and pathway analyses indicated that genes involved in wounding, inflammation and cell–extracellular matrix adhesion were upregulated, suggesting that suppression of these signaling pathways might also contribute to malignant phenotypes of MM cells by YAP activation, albeit their expressions might be indirectly suppressed (Supplementary Table 2).

YAP regulates CCND1 and FOXM1 transcription directly in cooperation with TEAD

Among the identified cell cycle regulatory genes, we focused on *CCND1*, a G1 cyclin-regulating RB/E2F pathway, and *FOXM1*, a transcription factor targeting both G1/S and G2/M progression regulators. *CCND1* and *FOXM1* were found to be commonly downregulated in the three cell lines from 0.13 to 0.48 and from 0.13- to 0.42-changes, respectively (Supplementary Table 1). Moreover, their promoter regions were also likely to harbor a putative recognition motif of TEAD, a transcriptional factor that binds to YAP.

To determine whether YAP regulates transcription of *CCND1* and *FOXM1* directly in MM cells, we carried out a chromatin immunoprecipitation assay. We prepared a primer set for the proximal promoter region of both genes to include the putative TEAD recognition motif[33] (Figure 2a). When precipitated with anti-YAP antibody, we detected positive PCR products of the proximal promoter regions of both genes, which indicated the direct binding of YAP to the *CCND1* and *FOXM1* proximal promoter regions (Figure 2b), although they were not detected in the distal regions (data not shown).

Next, to determine whether YAP induces transcription of *CCND1* and *FOXM1*, and then transcription is further enhanced

by exogenous TEAD transcription factor, we performed luciferase reporter assay for the promoter regions of these genes (Figure 2a) with YAP wild type and its constitutively active form, YAP S127A. We found that cotransduction of wild-type TEAD4 with YAP wild type or the active mutant form significantly induced both *CCND1* and *FOXM1* promoter activities. On the other hand, cotransduction of other mutant forms including YAP S94A[24] or TEAD4ΔCt,[34] both of which were thought to disrupt the YAP-TEAD interaction, did not show the enhancement of luciferase activity (Figures 2c and d).

These results provided support for the notion that *CCND1* and *FOXM1* might be the direct target genes of YAP in MM cells. Consistent with our observations, induction of *CCND1* by YAP has also been suggested by other studies. For example, in vertebrate neural tube development, YAP and TEAD promoted cell cycle progression by inducing *CCND1*.[21] As an upstream suppressive regulator of YAP, Merlin was also shown to inhibit *CCND1* expression by using *NF2*-deficient MM cells.[35] Although those reports did not refer to transcriptional regulation of *CCND1* by YAP, they demonstrated a contribution of Hippo signaling pathway to *CCND1* regulation, which our present findings corroborate.

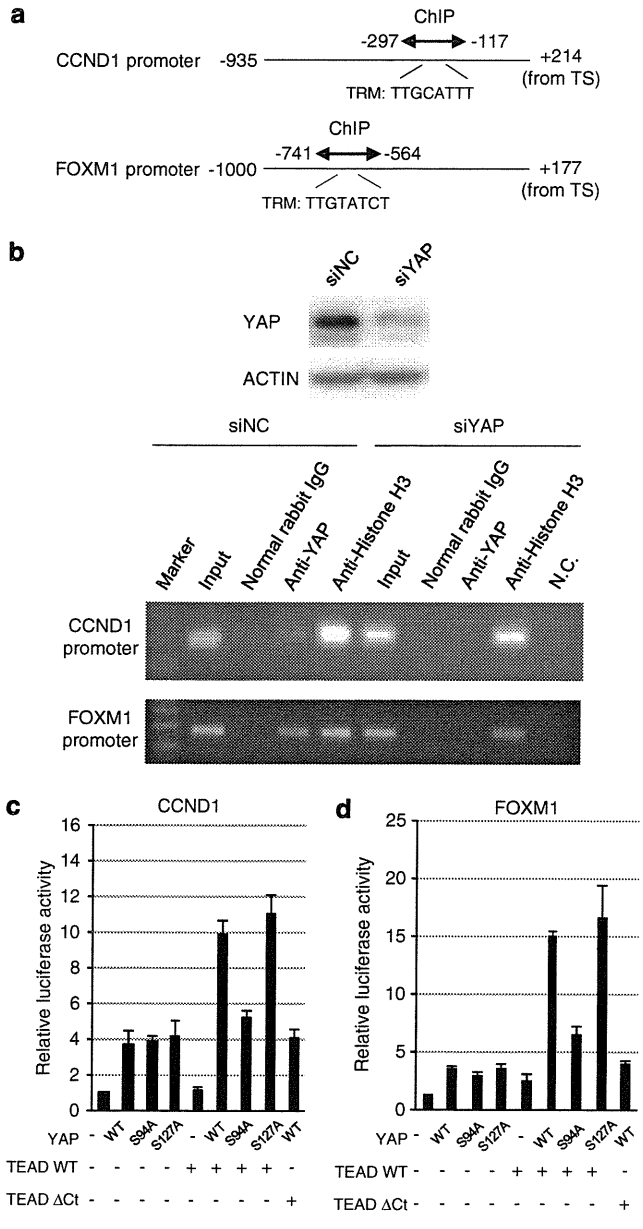

Figure 2. YAP directly induces transcription of the *CCND1* and *FOXM1* genes. (**a**) Each promoter includes the putative TEAD recognition motif (TRM), XDGHATXT, where X = A, T, C or G; D = A or T; and H = A, T or C. ChIP primer sets (arrow) were designed to include the motif. DNA fragments of nucleotide position −935 to +214 for *CCND1* and nucleotide position −1000 to +177 for *FOXM1* were inserted into luciferase reporter vectors. TS: transcriptional start. (**b**) ChIP assay using ChIP kit (ab500, Abcam) demonstrated that YAP bound to the *CCND1* and *FOXM1* proximal promoter regions. NCI-H290 cells treated with YAP siRNA (siYAP; Ambion, Austin, TX) were used as YAP-suppressed control, while cells with an irrelevant siRNA (siNC) maintained high YAP expression, as confirmed with western blot analysis. (Upper panel) After the cells with high or low YAP expression were subjected to immunoprecipitation assay with normal rabbit IgG (SC2027, Santa Cruz), rabbit anti-YAP antibody, or anti-H3 antibody (ab1791, Abcam) and protein A beads, immunoprecipitated chromatin were decross-linked. Recruited DNA was subjected to PCR using primer sets for proximal promoter regions of *CCND1* and *FOXM1*, and PCR products were electrophoresed in agarose gel. (Lower panel) Note that amounts of PCR products from the chromatin, which was precipitated with the anti-YAP antibody, were suppressed by pretreatment with siYAP. (**c, d**) For reporter assay, MeT-5A cells were transfected with the pGL3 basic firefly luciferase reporter plasmid with the *CCND1* or *FOXM1* promoter region by using FuGENE 6 transfection reagent (Roche, Mannheim, Germany). Renilla luciferase plasmid was also transfected for internal control. Thirty-six hours later, cells were lysed and subjected to dual-luciferase assay (TOYO INK, Tokyo, Japan). The promoter activities were enhanced with combined transduction of TEAD4 WT with wild type (WT) or constitutively activated forms of YAP (YAP S127A), but not with YAP S94A (inactive for TEAD binding) or TEAD4ΔCt (inactive for YAP binding) forms. Columns are the means of experiments, and bars represent s.d. (**c, d**).

YAP depletion suppressed cell cycle-promoting gene expressions in MM cells

The gene ontology analysis based on the microarray-based expression profiling suggested a significant contribution of YAP to the cell cycle process in MM cells. Based on our previous data indicating G1 cell cycle arrest in NCI-H290 cells by YAP knockdown,[17] we studied the status of cell cycle and expressions of cell cycle-promoting genes in a time-dependent manner after YAP-shRNA lentivirus infection. We found that G1 cell cycle arrest occurred at as early as 48 h, and the population of G1 cell cycle arrest increased at 72 h (Figure 3a). With quantitative real-time RT-PCR analysis, suppression of the *CCND1* gene expression was revealed to follow the downregulation of *YAP* as expected (Figure 3c). Consistent with the expression array analysis, other cell cycle-promoting genes including *E2F1, Aurora kinase B* (*AURKB*), *Polo-like kinase 1* (*PLK1*) and *NIMA-related kinase 2* (*NEK2*), also showed the decrease in the expression levels according to YAP-downregulation (Figure 3c). However, other irrelevant genes such as *SMAD3* did not show any decrease (data not shown). These results suggested that, together with YAP-direct target genes of *CCND1* and *FOXM1*, other cell-promoting genes are also involved in the dysregulated cell cycle machinery in YAP-activated MM cells.

Additionally, we observed that YAP-knockdown increased subG1 population of the cells in flow cytometric analysis (Figure 3b) and affected the expression levels of several apoptotic-related genes, including the downregulation of *BIRC5* (also known as *survivin*), an anti-apoptotic gene, and upregulated the one of *BCL2L11* (also known as *BIM*), a pro-apoptotic gene (Supplementary Table 2). In a flow cytometric assay with

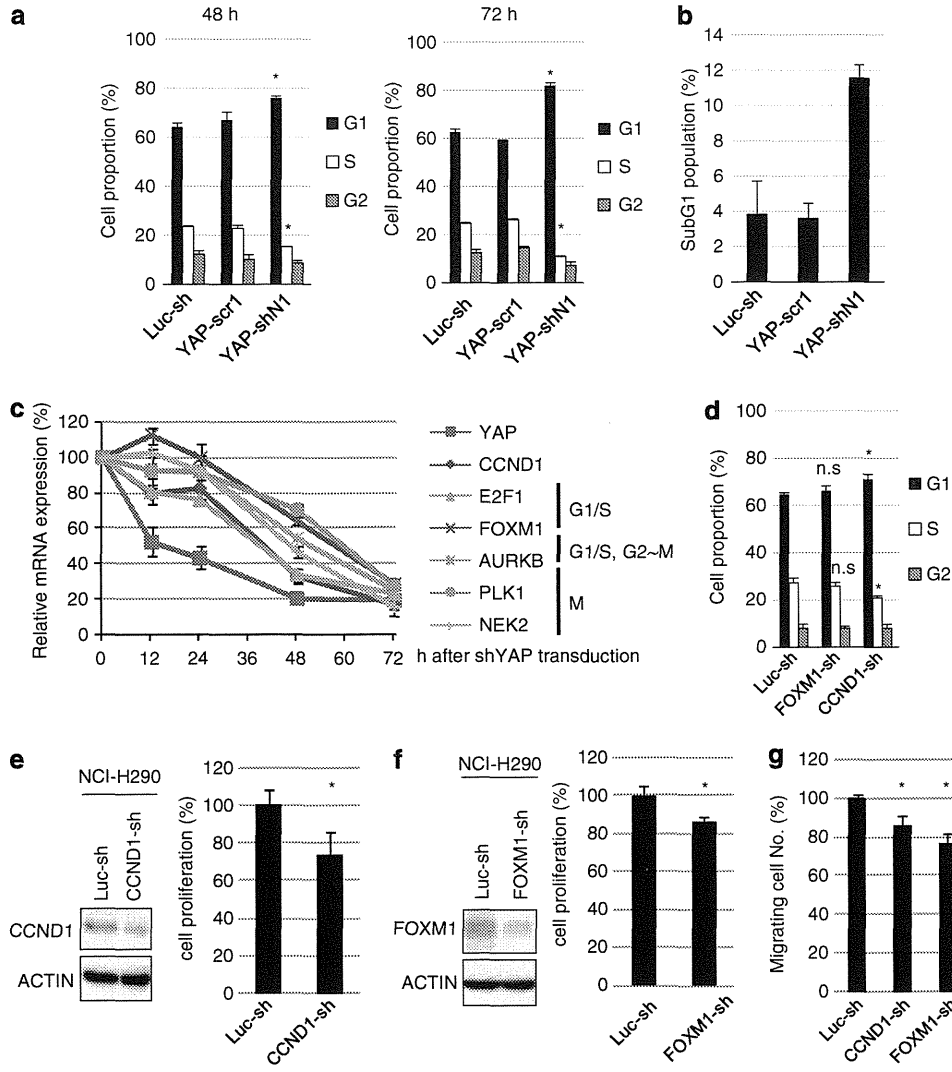

Figure 3. Involvement of YAP, CCND1 and FOXM1 in cell proliferation in NCI-H290 cells. (**a**) Flow cytometry analysis. After infection with YAP-shN1, YAP-scr1, or Luc-sh lentivirus, cells were incubated to grow for 48 or 72 h. Cells were harvested, washed with PBS and fixed with 70% ethanol. After treatment by RNaseA, cells were stained with propidium iodide (Sigma) and flow cytometry analysis was carried out. Cell cycle analysis revealed increased population of G1 phase and decreased population of S phase in NCI-H290 cells 48 h (left) and 72 h (right), respectively, after YAP-shN1 lentivirus infection. (**b**) YAP-knockdown induced subG1 population of MM cells. (**c**) Quantitative real-time RT-PCR analysis was performed with ABI 7500 Real-Time PCR System (Applied Biosystems, Foster, CA, USA). Glyceraldehyde-3-phosphate dehydrogenase (GAPDH) served as an endogenous control. The graph shows the changes in mRNA expression levels of cell cycle-related genes in response to YAP depletion. Symbols are the means of experiments normalized to control cell, and bars represent s.d. (**d**) Flow cytometry analysis. Knockdown of *CCND1* modestly increased the number of G1/S arrest cells in MM cells. (**e**, **f**) Cell proliferation assay. Knockdown of *CCND1* (**e**) and *FOXM1* (**f**) moderately suppressed cell proliferation in NCI-H290 cells. (**g**) Cell migration assay. Knockdown of *CCND1* and *FOXM1* induced modest suppression of NCI-H290 cell migratory activity. Columns are the means of experiments, and bars represent s.d. Asterisks represent $P<0.05$ between YAP-shN1 (**a**), CCND1-sh (**d**, **e**, **g**), or FOXM1-sh (**d**, **f**, **g**) versus Luc-sh control. n.s., not significant.

annexin V, a modest increase of early apoptotic cell population was also detected (Supplementary Figure 2). Although these data suggested apoptosis induction in MM cells, we did not find significant caspase activation with western blot analysis probably due to a relatively small population of MM cells that underwent apoptosis (data not shown). Thus, further studies may be warranted to clarify the underlying mechanism and significance of cell death by YAP-knockdown in MM cells.

CCND1 contributes to G1/S transition in MM cells

To determine whether knockdown of individual cell cycle specific genes regulated by YAP is sufficient to induce G1 cell cycle arrest in MM cells, we performed cell cycle analysis of NCI-H290 cells with knockdown of *CCND1* or *FOXM1*. After transduction of CCND1-sh, we found that the cell population of G1 phase increased and that of S phase decreased compared with the control cell (Figure 3d), although the effect was weaker than that of YAP-sh. However, the effect of FOXM1-sh on cell cycle progression was not clear (Figure 3d).

Finally, to evaluate proliferative roles of CCND1 or FOXM1 as YAP transcriptional targets in MM cells, we knocked down *CCND1* and *FOXM1* and performed proliferation analysis. The depletion of CCND1 and FOXM1 caused modest suppression compared with YAP depletion, though the decrease of proliferation was larger in CCND1 depletion than FOXM1 depletion at 26% and 14%,